Tree height uncertainty biases aboveground biomass estimation more than wood density in miombo woodlands

Arthur M. Yambayamba[1,2*], Ferdinand Handavu[3], Kondwani Kapinga[4,5], Tommaso Jucker[1]

Affiliations

[1]School of Biological Sciences, University of Bristol, Bristol, UK

[2]School of Natural Resources, Copperbelt University, Kitwe, Zambia

[3]Department of Geography, Environment and Climate Change, Mukuba University, Kitwe, Zambia

[4]Dag Hammarskjöld Institute for Peace and Conflict Studies (DHIPS), Environment, Sustainable Development and Peace, Copperbelt University, Kitwe, Zambia

[5]Chair of Environment and Development, Oliver R. Tambo Africa Research Chair Initiative (ORTARChI), Copperbelt University, P.O. Box 21692, Kitwe, Zambia

Corresponding author

Arthur M. Yambayamba, School of Biological Sciences, University of Bristol, 24 Tyndall Avenue, Bristol, BS8 1TQ, UK.

Email: arthur.yambayamba@bristol.ac.uk or ympazi@gmail.com

17 **ABSTRACT**

18 Accurate and unbiased estimation of tree aboveground biomass (*AGB*) is essential for large-
19 scale monitoring of forest carbon stocks. But estimating *AGB* typically requires several data
20 imputation steps that can introduce substantial errors that are hard to quantify and correct for.
21 Two sources of uncertainty that are thought to be particularly important but remain
22 understudied are tree height – which is generally estimated using allometric models – and wood
23 density – which is most commonly assigned from databases based on taxonomic matching.
24 Here we used data from 155 destructively harvested trees in Zambia's miombo woodlands that
25 span a large range of sizes to quantify errors in *AGB* arising from uncertainty in tree height and
26 wood density. We found that when locally-calibrated height-diameter allometries are used to
27 estimate missing tree height information and when wood density is imputed from species-
28 specific values derived from public databases, *AGB* can be estimated with high precision and
29 little or no bias. However, when tree height and wood density are imputed more coarsely using
30 data that are not biome specific, errors in *AGB* can be substantial. Specifically, estimating tree
31 height using a regional allometric model developed for tropical dry forests led to
32 underestimating *AGB* by 35%. Our study underscores the importance of accurately accounting
33 for tree height and wood density to estimate *AGB*, thereby paving the way for more robust
34 estimation of forest carbon stocks and their uncertainties across a range of ecosystem types.

35 **Key words**: forest carbon; destructive sampling; allometry; power law scaling; Bayesian
36 regression

1. INTRODUCTION

Forests and savannas play a crucial role in regulating the terrestrial carbon cycle by sequestering large amounts of carbon dioxide (CO_2) from the atmosphere and storing it as woody biomass (Rathgeber et al., 2016). This potential of forests to act as long-term carbon sinks, that slow the pace of climate change by partially offsetting anthropogenic CO_2 emissions, has gained widespread attention in recent decades (Grantham et al., 2020; Ellis et al., 2021; Arias et al., 2021). This has led to growing interest in restoration programs centered around forest creation and expansion (Lewis et al., 2019; Hua et al., 2024), as well as burgeoning international forest carbon markets underpinned by programs such as REDD+ (Bomfim et al., 2022) and dedicated satellite missions to map global forest carbon stocks (Quegan et al., 2019; Dubayah et al., 2020). However, a fundamental assumption of these efforts is that forest carbon stocks can be estimated accurately and without bias. In practice, this is rarely the case even at the most basic level of the individual tree (Demol et al., 2024; Fareed and Numata, 2024; Terryn et al., 2024), as there are multiple sources of uncertainty that affect tree biomass estimation and we lack a clear understanding of their relative importance and magnitude.

A fundamental unit of forest carbon stock estimation is a tree's aboveground woody biomass (*AGB*). Direct measurements of *AGB* involves destructive sampling to weigh the trunk and branches, which in addition to killing the tree is laborious and costly (Clark and Kellner, 2012; Colgan et al., 2013). In practice, *AGB* is therefore almost always estimated using allometric equations that have been calibrated using data from relatively small numbers of trees whose mass has been destructively measured (Chave et al., 2004) – although more recently terrestrial laser scanning is being increasingly used to generate accurate, non-destructive estimates of tree woody volume and *AGB* (Momo Takoudjou et al., 2018; Calders et al., 2022; Demol et al., 2024). These allometric biomass equations typically rely on some combination of stem diameter at breast height (D), tree height (H), wood density (ρ) and, in rarer cases,

crown width as input variables (Chave et al., 2014; Goodman et al., 2014; Ploton et al., 2016; Jucker et al., 2017). A myriad of such equations exist (Henry et al., 2013; Chojnacky et al., 2014; Zianis et al., 2005), but among the most widely used for tropical trees is the pantropical model developed by Chave et al. (2014), which express *AGB* as a power-law function of $D^2 \times H \times \rho$ – a compound variable that approximates a tree's trunk volume ($D^2 \times H$) and multiplies this by the density of its wood to estimate *AGB*.

However, the estimation of *AGB* using such models can be greatly impacted by the quality of measurements or imputation of the input variables. In particular, while *D* is generally recorded accurately and precisely in forest inventories, the same is not true for *H* and ρ. Common approaches to measuring *H* in the field using clinometers and laser range finders are both difficult to do accurately and time consuming. When *H* is measured directly in the field, estimates are therefore often uncertain and in some cases systematically biased (Larjavaara and Muller-Landau, 2013; Sullivan et al., 2018; Terryn et al., 2024), with the height of tall trees often underestimated. More commonly, *H* is not measured at all, but is instead itself estimated from *D* using allometric equations (Fayolle et al., 2016; Sullivan et al., 2018). These *H–D* allometries not only propagate any underlying biases in the *H* measurements used to parameterize them, but can also introduce additional sources of uncertainty that are hard to quantify once scaled to *AGB*. This includes errors arising from the choice of functional form used to model *H–D* allometries (Fayolle et al., 2016; Ledo et al., 2016; Cano et al., 2019; Terryn et al., 2024) and the fact that *H–D* scaling relationships can vary considerably among tree species and forest types (Feldpausch et al., 2011; Banin et al., 2012; Jucker et al., 2022; Jucker et al., 2025).

Similarly, ρ is very rarely measured as part of field inventories and is instead almost always assigned from global databases based on taxonomic or geographic matching (Chave et al., 2009; Réjou-Méchain et al., 2017; Fischer et al., 2026). While these databases are

87 invaluable, they still only cover <15% of known tree species, meaning that in many cases ρ is
88 imputed using either taxonomic (e.g., genus or family-level means) or geographic proxies (e.g.,
89 plot or regional-level means). Depending on a region's taxonomic coverage in the database and
90 the choice of imputation method, uncertainty in ρ can therefore substantially bias *AGB*
91 estimates (Flores and Coomes, 2011; Mitchard et al., 2014; Phillips et al., 2019).

92 Here we provide a rigorous quantitative assessment of how uncertainty in both *H* and
93 ρ propagates to tree-level *AGB* estimates, focusing specifically on southern Africa's miombo
94 woodlands. Like other tropical dry forests, miombo woodlands remain underrepresented in the
95 research and conservation agenda despite being among the most extensive tropical dry forests
96 in Africa and globally (around 2 million km^2; (Ribeiro et al., 2020)) and storing substantial
97 amounts of carbon in their vegetation (around 20–30 Mg C ha^{-1}; (Mcnicol et al., 2018)). To
98 address this knowledge gap, we compiled data for 155 trees whose *AGB* was measured via
99 destructive sampling in the miombo woodlands of Zambia. These trees cover a wide spectrum
100 of sizes (D = 5.0–68.2 cm; H = 2.9–25.0 m) and represent 37 uniquely identified species that
101 vary considerably in their wood density (ρ = 0.34–0.86 g cm^{-3}). Using these data, we set out to
102 address three research objectives:

103 (1) Compare the predictive performance of existing local and pantropical biomass models
104 that differ in their functional form;
105 (2) Reparametrize existing biomass models with new data to assess how this improves
106 their fit;
107 (3) Determine how different approaches to imputing H and ρ affect tree-level *AGB*
108 estimates.

109

2. MATERIALS AND METHODS

2.1 Study system

The study was conducted using datasets acquired in miombo woodlands from three sites in the Copperbelt Province of Zambia – Mwekera, Miengwe and Katanino (Fig. 1). Miombo woodlands are characterized by the dominance of trees in the genus *Brachystegia* that form open-canopy habitats where trees and grasses co-exist. Regionally, they cover around 2 million km^2 of land, forming a belt that stretches from Angola's Atlantic coast to the Indian Ocean in Mozambique and Tanzania (Dziba et al., 2020). Miombo woodlands are shaped by long dry seasons (5–8 months), followed by months of intense rainfall which usually falls between November and April. Annual rainfall varies considerably across the region, from around 1600 mm in norther Zambia and southern DRC to as little as 600 mm in Angola and southern Zambia (Ribeiro et al., 2020). Accordingly, the woodlands can be dividend into wet (>1000 mm) and dry miombo (<1000 mm), which differ in their structure and species composition (White, 1983). These woodlands are further shaped by human disturbances comprising mainly of fires, wood harvesting and land clearing for agriculture (Chidumayo, 2013a). Trees have evolved and adapted to these disturbances and recover remarkably quickly (Chidumayo, 2004; Syampungani et al., 2017), with aboveground carbon stocks returning to pre-disturbance levels in around 25–40 years (Williams et al., 2008; Mcnicol et al., 2015). However, regional aboveground carbon density estimates vary significantly among studies (15–72 Mg C ha^{-1} for mature woodlands; (Ribeiro et al., 2020)). While some of this variation reflects differences in climate, species composition and disturbance regimes (Handavu et al., 2021), it also arises from differences in the way *AGB* is estimated (Demol et al., 2024). This underscores the importance of resolving these sources of uncertainty to improve regional carbon stock estimates.

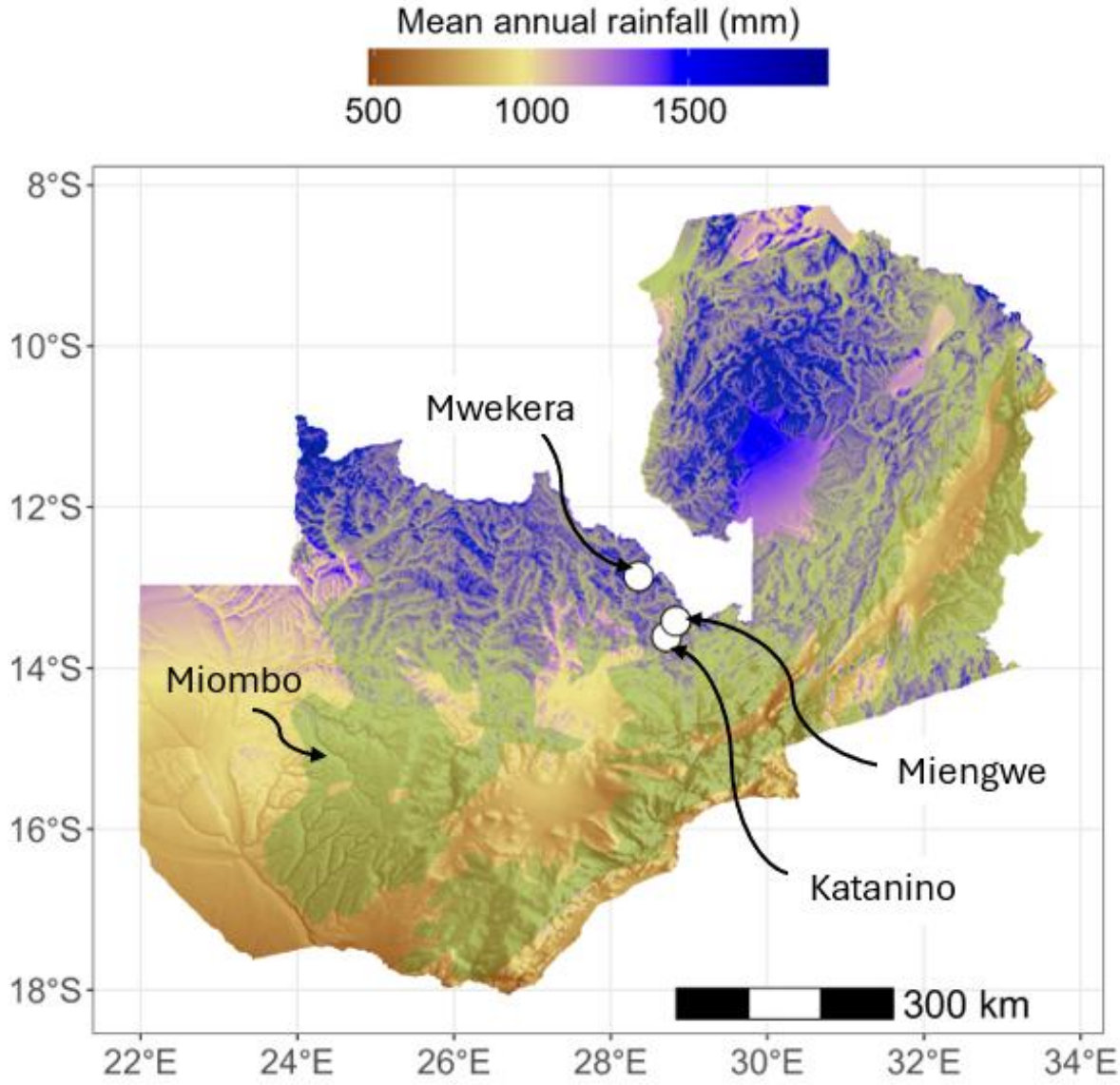


Figure 1. A map of Zambia showing the extent of the miombo woodlands (green shading) and the location of the three sites (white filled circles) from where the data used in the study were collected. The distribution of mean annual precipitation across the country shows the approximate locations of wet miombo (northern part) and dry miombo (southern part) within Zambia. Precipitation data was extracted from the CHELSA-BIOCLIM+ database at a spatial resolution of 30 arc-seconds (approximately 1 km) (Brun et al., 2022). The shapefile for miombo woodlands extent was obtained from Poppenwimer (2022) based on the description of ecoregions by Olson et al. (2001).

142 **2.2 Tree harvest data**

143 We compiled three separate datasets for which a combined total of 158 individual trees
144 belonging to 37 tree species were destructively harvested to measure *AGB*. Prior to conducting
145 destructive sampling, vegetation surveys were conducted to assign trees to different *D* classes
146 (minimum *D* = 5 cm) from which a random subset was selected for harvesting. In all the three
147 sites, *D* was measured to the nearest 0.1 cm using diameter tapes while *H* was measured using
148 either a Suunto hypsometer (before trees were felled, at the Mwekera) or a 50 m measuring
149 tape (after felling trees at the other two sites). Selected trees were felled at ground level (<15
150 cm from the ground) and then cut into manageable segments of between 1–3 m using chain
151 saws. The cut segments were then weighed for fresh mass in the field using the END-T3
152 weighing indicator with a capacity of 600 kg and a precision of 0.01 kg. Furthermore, all small
153 branches, twigs and leaves were cut from each trunk and measured for mass (Kapinga et al.,
154 2018; Handavu et al., 2021).

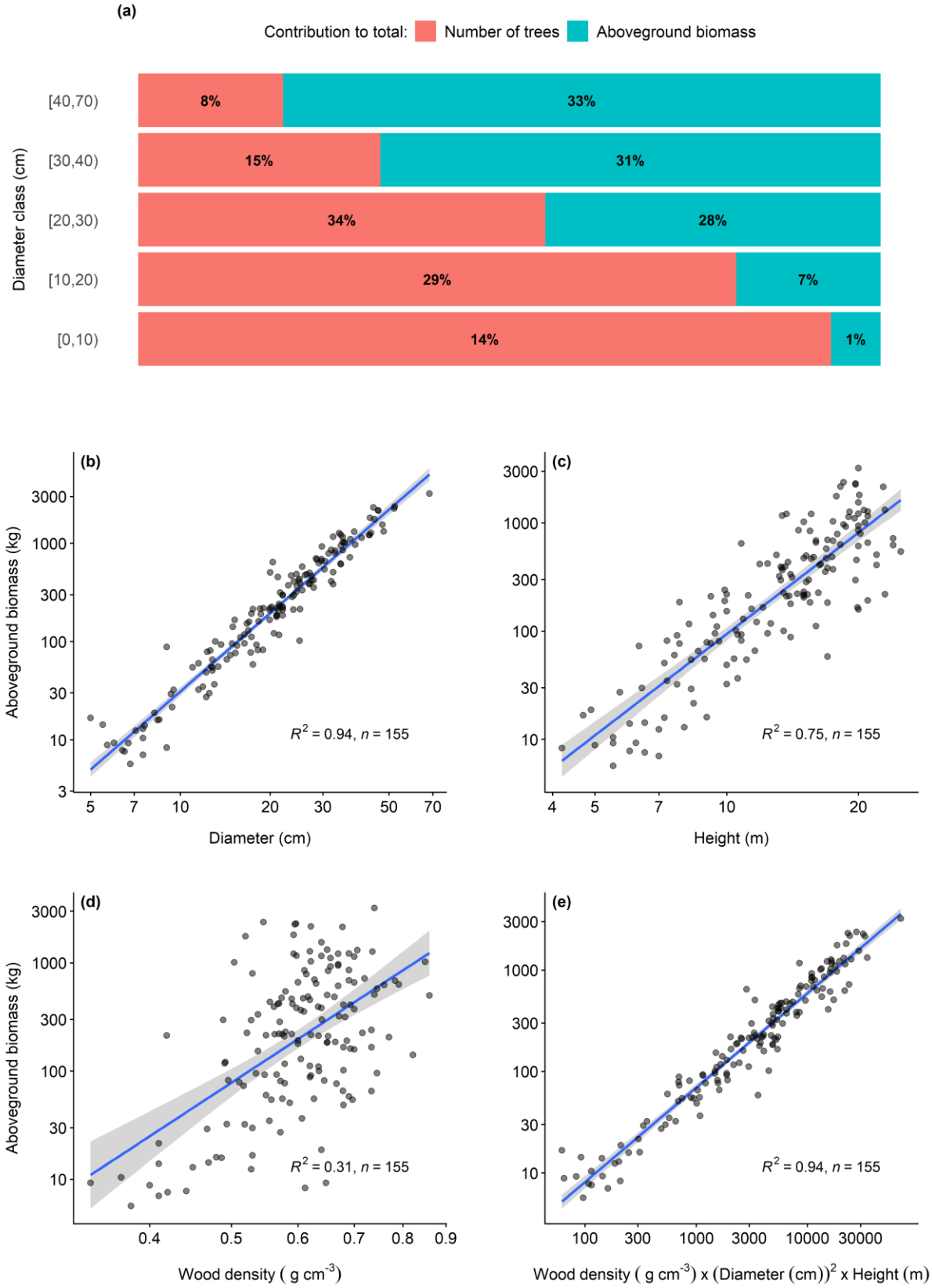
155 In addition to *AGB*, *D*, and *H*, the wood density (ρ, in g cm^{-3}) for each tree was also
156 measured. Specifically, ρ was determined using sample discs cut from all wood components
157 (trunk base, trunk segments, large and small branches) to account for variation in ρ within a
158 tree. The cut discs were taken to the laboratory where they were oven dried at 105°C for 48
159 hours and then mass was determined using a scale with precision of 0.001 g. The oven dried
160 discs were then submerged in water for 48 hours to reach saturation before determining the
161 volume of green (fresh) wood. The volume for each disc was determined using the water
162 displacement method using graduated cylinders. ρ was then calculated as the oven dry mass
163 per unit volume of green wood (Kapinga et al., 2018; Handavu et al., 2021).

164 To rule out potential measurement errors that could unduly influence the calibration of
165 *AGB* models, we used Cook's distance and studentized residuals to check for outliers in the
166 bivariate relationship between *AGB* and *D* (on a log-log scale). Based on this, we identified

three data points that were flagged as outliers and excluded from further analysis (Fig. S1a). This left us with 155 trees for comparing and reparametrizing *AGB* models. This dataset covered a large spectrum of sizes (D = 5.0–68.2 cm; H = 4.2–25.0 m), with *AGB* ranging between 5.7–3209.9 kg and wood density ranging between 0.34–0.86 g cm^{-3} (Table 1 and see Fig. 2 for a summary of the tree harvest data and the relationship between *AGB* and its predictors).

Table 1. Breakdown of the tree harvest dataset for the three sites in miombo woodlands, including number of trees harvested and species, as well as the median and range (in square brackets) of stem diameter at breast height, total tree height, wood density, aboveground biomass, elevation, mean total annual precipitation and mean annual temperature.

	Katanino forest	**Miengwe forest**	**Mwekera forest**	**Combined dataset**
Number of trees harvested	12	94	49	155
Number of species	9	33	5	37
Stem diameter (D; cm)	22.6 [12.2 – 46.0]	21.3 [5.0 – 52.2]	22.0 [5.5 – 68.2]	21.4 [5.0 – 68.2]
Tree height (H; m)	13.5 [5.7 – 22.8]	12.9 [4.2 – 20.7]	17.0 [5.0 – 25.0]	13.8 [4.2 – 25.0]
Wood density (ρ; g cm^{-3})	0.64 [0.49 – 0.86]	0.60 [0.42 – 0.82]	0.64 [0.34 – 0.85]	0.61 [0.34 – 0.86]
Aboveground biomass (*AGB*; kg)	301.0 [27.2 - 2149.3]	217.7 [7.8 - 2374.4]	230.6 [5.7 – 3209.9]	219.2 [5.7 – 3209.9]
Mean elevation (m a.s.l.)	1323	1324	1228	[1228 – 1324]
Mean annual precipitation (mm yr^{-1})	1325	1250	1198	[1198 – 1325]
Mean annual temperature (°C)	20.1	20.2	20.9	[20.1 – 20.9]



178

179 **Figure 2.** Overview of the tree harvest dataset. The bar plot **(a)** shows the distribution of

180 samples across the five tree diameter classes in terms of both number of trees and their

contribution to above ground biomass (*AGB*), both expressed as percentages of the total – Note that the bars in **(a)** are not plotted to scale but merely show the percentage contribution of each *D* class to total number of trees and total *AGB*. Scatterplots show the relationship between *AGB* and the predictors used to model it, including **(b)** stem diameter (*D*), **(c)** total tree height (*H*), **(d)** wood density (ρ) and **(e)** the compound variable of *D*, *H* and ρ. The coefficient of determination (R^2) between *AGB* and each of the predictor variables is shown along with the line of best fit (blue colour) and its 95% confidence bound (grey colour). The dark grey filled circles represent the *AGB* values of each of the 155 destructively harvested trees, plotted on a log-log scale.

Apart from the tree harvest datasets used here, there are a number of other studies where destructive sampling for *AGB* has been conducted across miombo woodlands, including those in Mozambique (Ryan et al., 2011; Guedes et al., 2018), Malawi (Kachamba et al., 2016; Kuyah et al., 2016), Tanzania (Chamshama et al., 2004; Mugasha et al., 2013) and Zambia (Chidumayo, 2013b). However, all these datasets lack wood density measurements at the individual tree level and were therefore not suitable to address the core questions of our research.

2.3 Height–diameter modelling data

To determine how different approaches to imputing missing tree height values impact *AGB* estimates, we compiled an additional dataset of trees from miombo woodlands in Zambia for which both *H* and *D* were measured in the field. This included forest inventory data from the three study sites (Mwekera, Miengwe and Katanino) where trees were also destructively harvested to measure *AGB* (Kapinga et al., 2018; Handavu et al., 2021). In Mwekera, 16 square plots (25×25 m) were laid out and all trees with $D \geq 5$ cm in each quadrat were identified to species level. For each tree, *D* was measured to the nearest 0.1 cm using a diameter tape while *H* was measured to the nearest 0.1 m using a Suunto hypsometer (Kapinga et al., 2018). The

same forest inventory approach was used in Miengwe and Katanino forests, although in these two sites circular plots with a 20 m radius were used instead (Handavu et al., 2021). Collectively, *H* and *D* were measured for a total of 4410 trees – excluding the 155 trees which were harvested for *AGB*.

We assessed the data for potential outliers by fitting a log-log linear model relating *H* and *D*. Based on the Cook's distance, a total of 223 trees were flagged as likely measurement errors and were thus excluded from further analysis (Fig. S1b). This left us with 4187 trees for *H-D* model fitting, belonging to 79 tree species and spanning a similar range of tree sizes to those sampled for *AGB* (*D* = 5.0–70 cm; *H* = 2.9–33.0 m) (Table 2).

Table 2: Breakdown of the height-diameter modelling dataset for the three sites in wet miombo woodlands, including number of plots, trees measured, species as well as the median and range of stem diameter at breast height, total tree height, basal area, tree density, elevation, mean total annual precipitation and mean annual temperature. Climate data were extracted from the CHELSA-BIOCLIM+ database (Brun et al., 2022) at a spatial resolution of 30 arc-seconds (approximately 1 km).

Variable	Katanino forest	Miengwe forest	Mwekera forest	Combined dataset
Number of plots	7	55	16	-
Number of trees measured	208	3630	349	4187
Number of species	40	74	33	79
Stem diameter (*D*; cm)	16.0 [5.5 – 51.0]	13.4 [5.0 – 70.0]	20.5 [5.0 – 62.3]	14.0 [5.0 – 70.0]
Tree height (*H*; m)	10.0 [3.3 – 22.0]	9.8 [2.9 – 33.0]	12.5 [3.0 – 25.0]	10.0 [2.9 – 33.0]
Basal area (*BA*; $m^2\ ha^{-1}$)	12.0 [4.9 – 14.8]	15.5 [9.4 – 31.1]	18.1 [10.7 – 29.1]	15.5 [4.9 – 31.1]
Tree density (stems ha^{-1})	342 [104 – 414]	580 [287 – 1329]	416 [224 – 512]	565 [104 – 1329]
Elevation (m a.s.l)	1323 [1255 – 1327]	1324 [1286 – 1340]	1228	1323 [1228 – 1340]
Mean annual precipitation (mm yr^{-1})	1325 [1186 – 1353]	1250 [1130 – 1348]	1198	1249 [1130 – 1353]
Mean annual temperature (°C)	20.1 [20.1 – 20.4]	20.2 [20.1 – 20.5]	20.9	20.2 [20.1 – 20.9]

2.4 Data harmonization and analysis

All data processing and statistical analyses were conducted in R (version 4.3.1; (R Core Team, 2023)) using the brms, GGally, geodata, terra, tidyverse, data.table, ggpmisc, cowplot, multcompView, BIOMASS, rWCVP and U.Taxonstand packages (Bürkner, 2017; Réjou-Méchain et al., 2017; Wickham et al., 2019; Wilke, 2020; Schloerke et al., 2021; Hijmans, 2023; Dowle and Srinivasan, 2023; Brown et al., 2023; Zhang and Qian, 2023; Aphalo, 2024). Prior to conducting statistical analyses, we used the rWCVP and U.Taxonstand packages to harmonize tree species names across all datasets using the World Checklist of Vascular Plants (Govaerts et al., 2021; Brown et al., 2023). For this step, we also cross-referenced and matched species names against the Global Wood Density Database (GWDD) which we used in subsequent analyses to assign ρ values to species using the BIOMASS package (Chave et al., 2009; Réjou-Méchain et al., 2017).

2.5 Objective 1 – Comparing the performance of existing *AGB* models

To determine how much tree-level *AGB* estimates are influenced by the choice of biomass equation, we calculated and compared *AGB* estimates obtained using two existing biomass models. The first *AGB* equation we tested is one of most commonly used pantropical models developed by (Chave et al., 2014), which expresses *AGB* as the following function of *D*, *H* and ρ:

$$AGB = 0.067 \times (\rho D^2 H)^{0.976} \times \exp\left[\frac{0.357^2}{2}\right]. \quad (1)$$

where $\exp\left[\frac{0.357^2}{2}\right]$ is the Baskerville correction factor defined as $\frac{\hat{\sigma}^2}{2}$, with $\hat{\sigma}$ corresponding to the estimated residual standard error of the model. The correction factor is used to account for the systematic bias introduced when back-transforming from a log-log linear model to a power law function (Baskerville, 1972). This model was developed using a large collection of tree harvest data (4004 trees) from across the tropics, including the miombo. It has been used to

estimate *AGB* in tropical forests, including the miombo woodlands of Zambia (Pelletier et al., 2018; Kanja et al., 2025).

The second literature model we considered is a local *AGB* model developed as part of Zambia's second integrated land-use assessment (ILUA2) which estimates *AGB* from *D* alone (ILUA, 2016; Forestry Department, 2016):

$$AGB = 0.128 \times D^{2.342} \quad (2)$$

As mentioned previously, there are other *AGB* models developed from destructive samples across miombo woodlands, but for the purpose of this study, we chose eq. 2 for two reasons. First, the model was developed using one of the largest collated tree harvest datasets in the region: 1319 harvested trees in Botswana, Tanzania and Zambia. The trees were harvested in *Acacia*, mopane and miombo vegetation types but with the majority of trees (~85%) coming from dry and wet miombo (Forestry Department, 2016). To our knowledge, all the other existing models developed from destructive samples in the miombo are based on much smaller sample sizes (20–170 harvested trees). Second, this model has been adopted for use at national level in Zambia to estimate *AGB* for all vegetation types (ILUA, 2016), including to generate Zambia's forest reference emission level (FREL) submission to the United Nations Convention for Climate Change (UNFCC) (GRZ, 2016, 2021).

We used eqs. (1) and (2) to estimate the *AGB* for each of the 155 trees using measurements of *D*, *H* and ρ as inputs. We then compared the predictive ability of these two models on the basis of the root mean square error (RMSE, in kg) as a measure of precision, and percentage error (PE, in %) as a measure of bias:

$$\text{RMSE} = \sqrt{\left[\frac{1}{n}\sum_{i=1}^{n}\left(AGB_i - \widehat{AGB_i}\right)^2\right]} \quad (3)$$

$$\text{PE} = \left(\left(\frac{1}{n}\sum_{i=1}^{n}\left(\widehat{AGB_i} - AGB_i\right)\right) / \frac{1}{n}\sum_{i=1}^{n}(AGB_i)\right) \times 100 \quad (4)$$

where AGB_i is the measured AGB for tree i and $\widehat{AGB_i}$ is the predicted AGB for tree i.

We used PE to estimate the magnitude of the mean error relative to the mean observed *AGB*. We chose PE among other metrics of model performance because it gives more weight to large trees, which are the biggest source of uncertainty in *AGB* estimation and contribute disproportionately towards total forest carbon stocks (Fig. 1a; Lutz et al., 2018; Calders et al., 2022).

Finally, we also assessed the performance of the models by fitting a linear regression between observed and predicted *AGB* values and extracting the intercept and slope parameters with their associated 95% confidence intervals. If the model is unbiased, we would expect the intercept to have a value close to 0 and the slope to be approximately 1 (Sileshi, 2014).

2.6 Objective 2 – Reparametrizing *AGB* models to compare their performance to published equations

To complement the two existing *AGB* models, we used the tree harvest dataset described above to reparametrize a miombo-specific version of eqs. 1 and 2. Specifically, we fit linear regressions to log-log transformed data to model the power law relationship between *AGB* and either $\rho D^2 H$ or D alone. Models were fit in a Bayesian framework using the brms package. We used weak priors for the normalization constant (intercept) and scaling exponent (slope), which we assumed to be normally distributed. Parameter estimates were based on 6000 posterior samples drawn from 4 parallel chains after discarding 1000 burn-in draws per chain. Models were assessed based on the Gelman-Rubin statistic (Rhat = 1.00), the Bulk_ESS and Tail_ESS statistics (both >1000), and posterior predictive checks (Fig. S2), all of which confirmed that the models adequately converged and fitted the observed data well (see Appendix S1 for additional details on model fitting and validation). The resulting fitted models were as follows:

$$AGB = 0.119 \times (\rho D^2 H)^{0.923} \times \exp\left[\frac{0.373^2}{2}\right] \quad (5)$$

$$AGB = 0.083 \times D^{2.590} \times \exp\left[\frac{0.384^2}{2}\right] \quad (6)$$

289 Having reparametrized the two literature *AGB* models (eqs 1 and 2), we then compared
290 the performance of the four equations (1–2 and 5–6) based on RMSE and PE. This allowed us
291 to determine which of the two functional forms is most suitable for predicting *AGB* estimation
292 in miombo woodlands.

293 **2.7 Objective 3 – Influence of height and wood density uncertainty on *AGB* estimates**

294 To better understand how different approaches to imputing H and ρ impact tree-level *AGB*
295 estimates, we devised a series of scenarios in which we imputed values of H and ρ following
296 commonly used practices for dealing with missing data and quantified their relative
297 contribution to *AGB* errors. For the purposes of this analysis, we used the pantropical model of
298 (Chave et al., 2014) to predict *AGB* (eq. 1) since it performed well on our dataset (see Results
299 for details) and is widely used by the research community. As above, model performance was
300 assessed by comparing predicted and observed *AGB* values on the basis of RMSE and PE for
301 the entire dataset, as well as PE when grouping trees into different D size classes (<10 cm, 10–
302 20 cm, 20–30 cm, 30–40 cm, >40 cm).

303 As a starting point, we began by using eq. 1 to predict the *AGB* of all the 155 harvested
304 trees when using field-measured values of both H and ρ as inputs. This served as our best case
305 scenario, in which all inputs data have been directly measured in the field. Next, we repeated
306 this same process but replaced field-measured H values with estimates derived from two
307 alternative *H–D* allometries: (1) a locally-calibrated, species-specific allometry and (2) a
308 regional, biome-specific allometry. The local allometry was derived using H and D values from
309 the 4187 trees described above. The relationship was modelled as a power-law function fit to

log–log transformed data ($H = \alpha_j \times D^{\beta_j}$), where both the scaling coefficient (α, intercept) and scaling exponent (β, slope) were allowed to vary across species (j, 79 species + 1 group for 21 trees with no species identification) in a hierarchical Bayesian framework. Model fitting and assessment followed the same procedures described above for the reparametrized *AGB* models. Estimated species-level parameters are reported in Table S4, while the population-level fit (or fixed effects) was:

$$H = 1.846 \times D^{0.613} \times \exp\left[\frac{0.240^2}{2}\right] \quad (7)$$

For the regional *H–D* allometry, we used an existing model for tropical dry forest trees developed using the Tallo database (Jucker et al., 2022):

$$H = 2.355 \times D^{0.477} \quad (8)$$

Finally, we used a similar approach to vary the wood density inputs in the *AGB* equation. Specifically, we replaced field-measured ρ values with either (1) species-specific mean values (or closest taxonomic unit) obtained from the GWDD using the BIOMASS package (Réjou-Méchain et al., 2017) or (2) with a regional mean value for African tropical forests (ρ = 0.598 g cm^{-3}; (Chave et al., 2009). When matching to the GWDD, 55% of trees were assigned species-level values, 43% genus-level means and the remaining 2% a mean of the dataset (0.682 g cm^{-3}).

In total, this gave us nine scenarios to compare: three possible *H* inputs into the *AGB* equation (field-measured, species-specific or biome-specific), three possible wood density inputs (field-measured, species-specific or biome-specific), and their respective combinations (Table 3).

Table 3: Summary of the nine scenarios used to determine the impact of different height and wood density inputs when estimating AGB. Uncertainty, in AGB estimates, increasing from left to right for height inputs and from top to bottom for wood density.

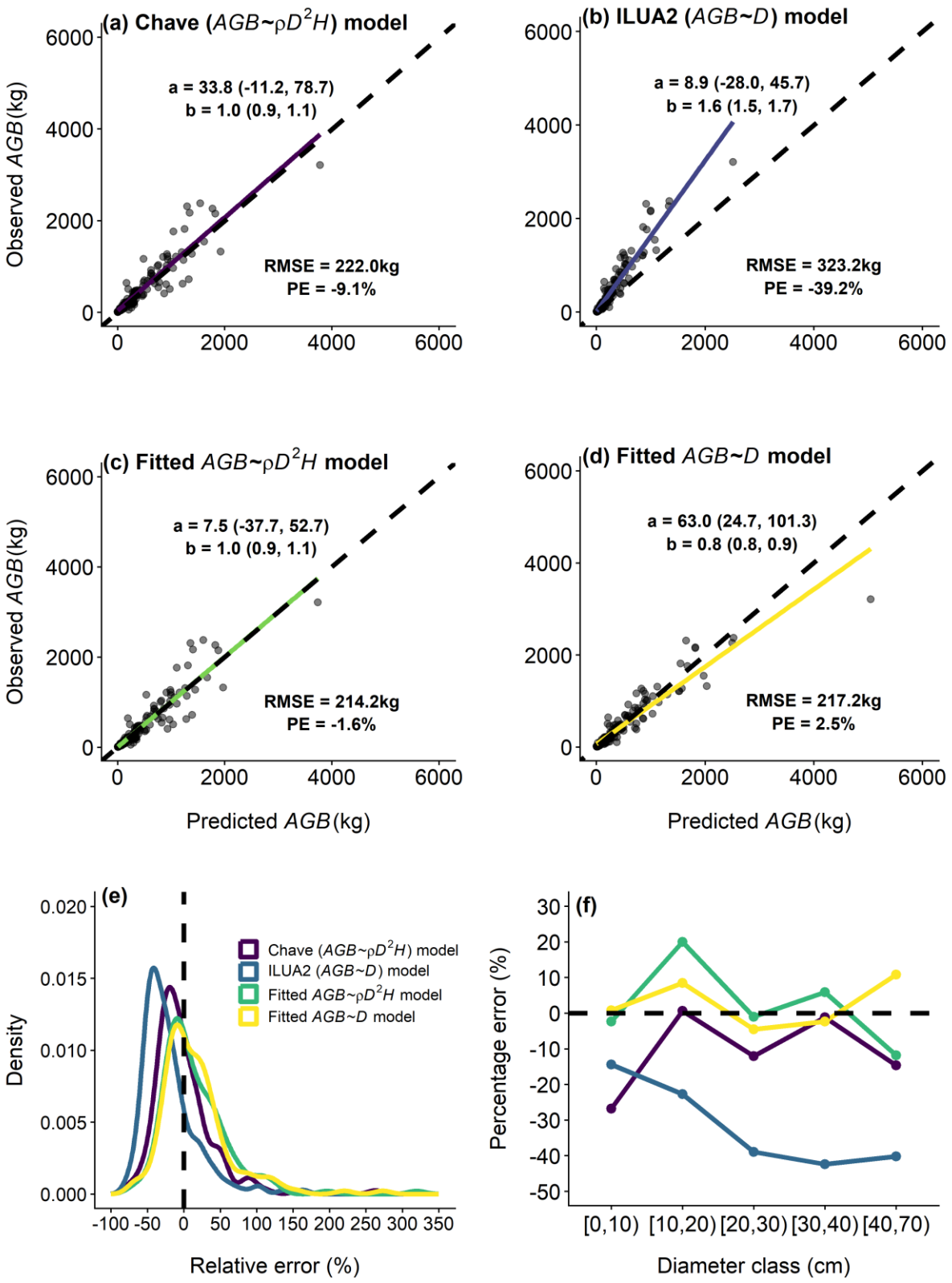
Scenario 1 Height: measured Wood density: measured Uncertainty: low	**Scenario 2** Height: species-specific *H-D* Wood density: measured Uncertainty: medium	**Scenario 3** Height: regional *H-D* Wood density: measured Uncertainty: medium-high
Scenario 4 Height: measured Wood density: species-specific from GWDD Uncertainty: medium	**Scenario 5** Height: species-specific *H-D* Wood density: species-specific from GWDD Uncertainty: medium-high	**Scenario 6** Height: regional *H-D* Wood density: species-specific from GWDD Uncertainty: high
Scenario 7 Height: measured Wood density: regional mean Uncertainty: medium-high	**Scenario 8** Height: species-specific *H-D* Wood density: regional mean Uncertainty: high	**Scenario 9** Height: regional *H-D* Wood density: regional mean Uncertainty: very high

3. RESULTS

3.1 Objectives 1 and 2 – Uncertainty in *AGB* estimation due to choice of *AGB* model

Of the four *AGB* models we compared, three performed similarly well and produced unbiased estimates of *AGB* across the range of tree sizes (Fig. 3 and Fig. S4): the two models calibrated using the tree harvest data presented in this paper (eqs. 5 and 6) and the existing pantropical model developed by Chave et al. (2014) (eq. 1). In particular, regressions between predicted and observed *AGB* values for both models that used $\rho D^2 H$ as predictors (eqs. 1 and 5) had intercepts with 95% confidence intervals that overlapped with 0 and slopes equal to 1. Of the three *AGB* models that performed similarly well, the reparametrized model with $\rho D^2 H$ as a predictor of *AGB* model had the lowest RMSE (214.2 kg) and PE (-1.6%; Fig. 3c). By contrast,

345 the ILUA2 model (eq. 2) developed as part of Zambia's forest inventory program substantially
346 underestimated *AGB* and had the worst performance metrics (RMSE = 323.2kg and PE = -
347 39.2%) (Fig. 3b), especially for large trees (blue line in Fig. 3f; see also Fig. S4). On average,
348 predicted values of *AGB* obtained using the ILUA2 model were around 35% lower than those
349 measured in the field (slope coefficient = 1.6; Fig. 3b) and trees in the largest size class had a
350 PE of -40% (Fig. 3f).



351

352 **Figure 3.** Predictive accuracy of the four alternative aboveground biomass (*AGB*) models.

353 Scatterplots **(a–d)** show the relationship between observed and predicted *AGB* values across

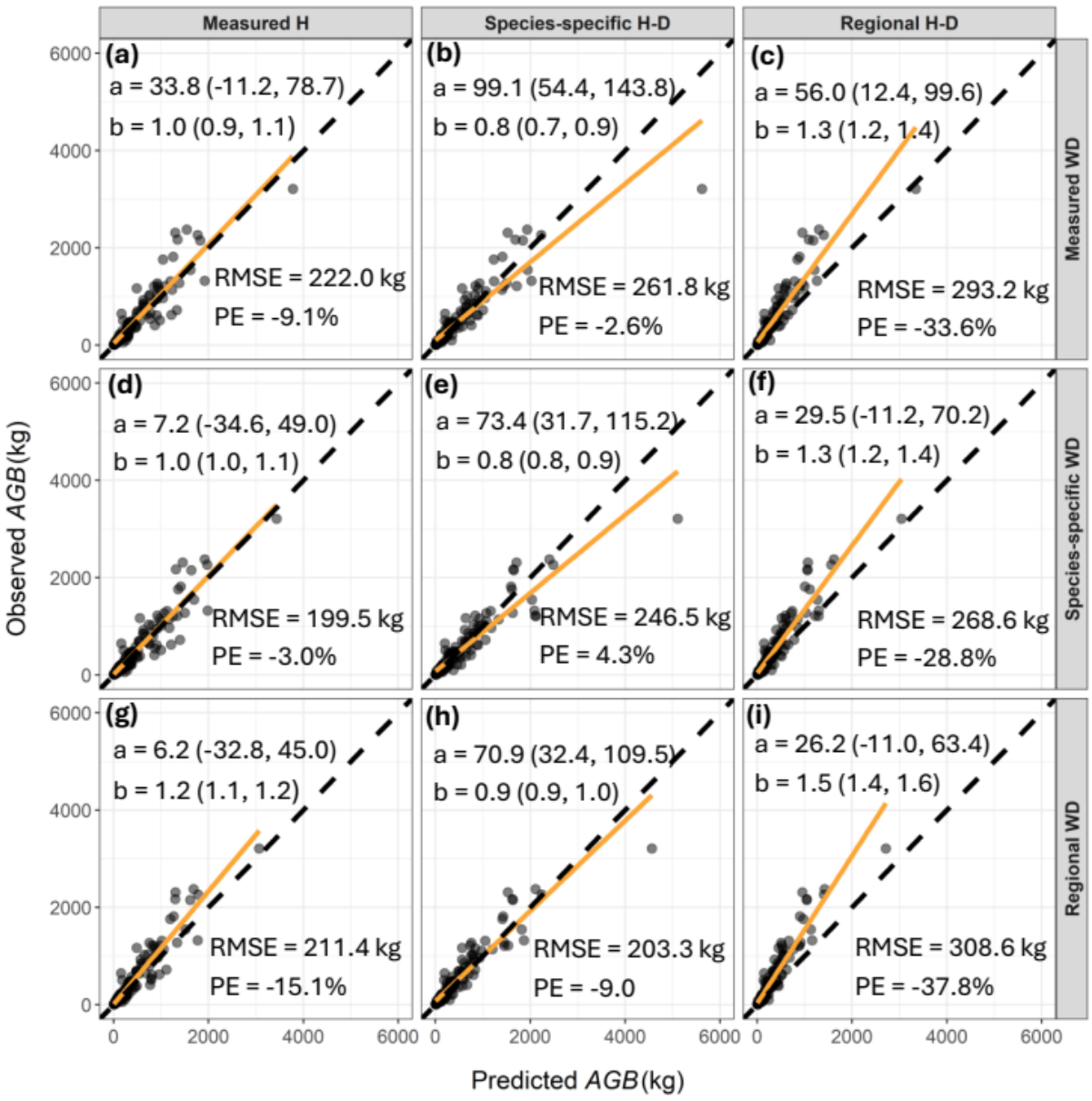
354 the 155 trees included in the dataset. Coloured lines correspond to the fit of a linear model
355 between observed and predicted *AGB* values, while dashed lines illustrate a 1:1 relationship.
356 Fit statistics for each model are reported in the panels, including the intercept, **a**, and slope ,**b**,
357 of the regression line with 95% confidence intervals in brackets. Model errors are visualised in
358 the bottom two panels, including **(e)** the distribution of relative errors, as a percentage,
359 (calculated as: $((\widehat{AGB}_i - AGB_i)/AGB_i) \times 100$; where AGB_i is the measured AGB for tree i;
360 and $\widehat{AGB}_i$ is the estimated AGB for tree i) for each of the four models and (**f**) the percentage
361 error (PE, in %) of trees grouped into five stem diameter classes.

362 **3.2 Objective 3 – Error in *AGB* estimation due to uncertainty in height and wood**
363 **density**

364 Across the nine scenarios in which we modified height (H) and wood density (ρ) inputs in the
365 pantropical *AGB* model, we found that replacing field-measured values of H and ρ with species-
366 specific estimates did not substantially worsen *AGB* estimates (Figs 4–5). In particular, height
367 estimates obtained using the locally-calibrated, species-specific *H–D* allometry (eq. 7) were
368 statistically indistinguishable (Fig. S5a) from those measured in the field and consequently had
369 little impact on predicted *AGB* values (PE = -2.6% and RMSE = 261.8 kg; Fig. 4b). Similarly,
370 while species-specific wood density values obtained from the GWDD were significantly higher
371 (Fig. S5b) than those measured on the destructively harvested trees, their use in the *AGB* model
372 had almost no impact on *AGB* estimation (PE = -3.0% and RMSE = 199.5 kg, with a slope
373 coefficient of 1.0 when comparing predicted and observed values of *AGB*; Fig. 4d).

374 By contrast, when H and ρ values were replaced with coarser regional-level estimates,
375 errors in *AGB* increased substantially. This was most pronounced for scenarios that involved
376 using height estimates derived from the regional *H–D* allometry for tropical dry forests (eq. 8;
377 Fig. 4c,f,i). Because this allometry severely underestimated tree heights by several meters

(Figs. 6 and S6), its use led to a nearly 35% underestimation of *AGB* (slope coefficient between observed and predicted values = 1.3; Fig. 4c). A similar, albeit much weaker trend was also observed for wood density. The regional mean ρ value for African tropical forests was only slightly lower than the mean ρ value of species sampled in our study (0.598 vs 0.607 g cm^{-3}). Therefore, replacing field-measured ρ values with a regional mean resulted in a slight increase in underestimation of *AGB* (PE = -15.1% and slope coefficient = 1.2; Fig. 4g). When these two sources of errors were combined, they compounded each other and led to an underestimation of *AGB* that was comparable in magnitude to that of using the ILUA2 model to estimate *AGB* instead of the pantropical equation of Chave et al. (2014) (PE = -37.8%, RMSE = 308.6 kg and slope coefficient = 1.5; Fig. 4i).

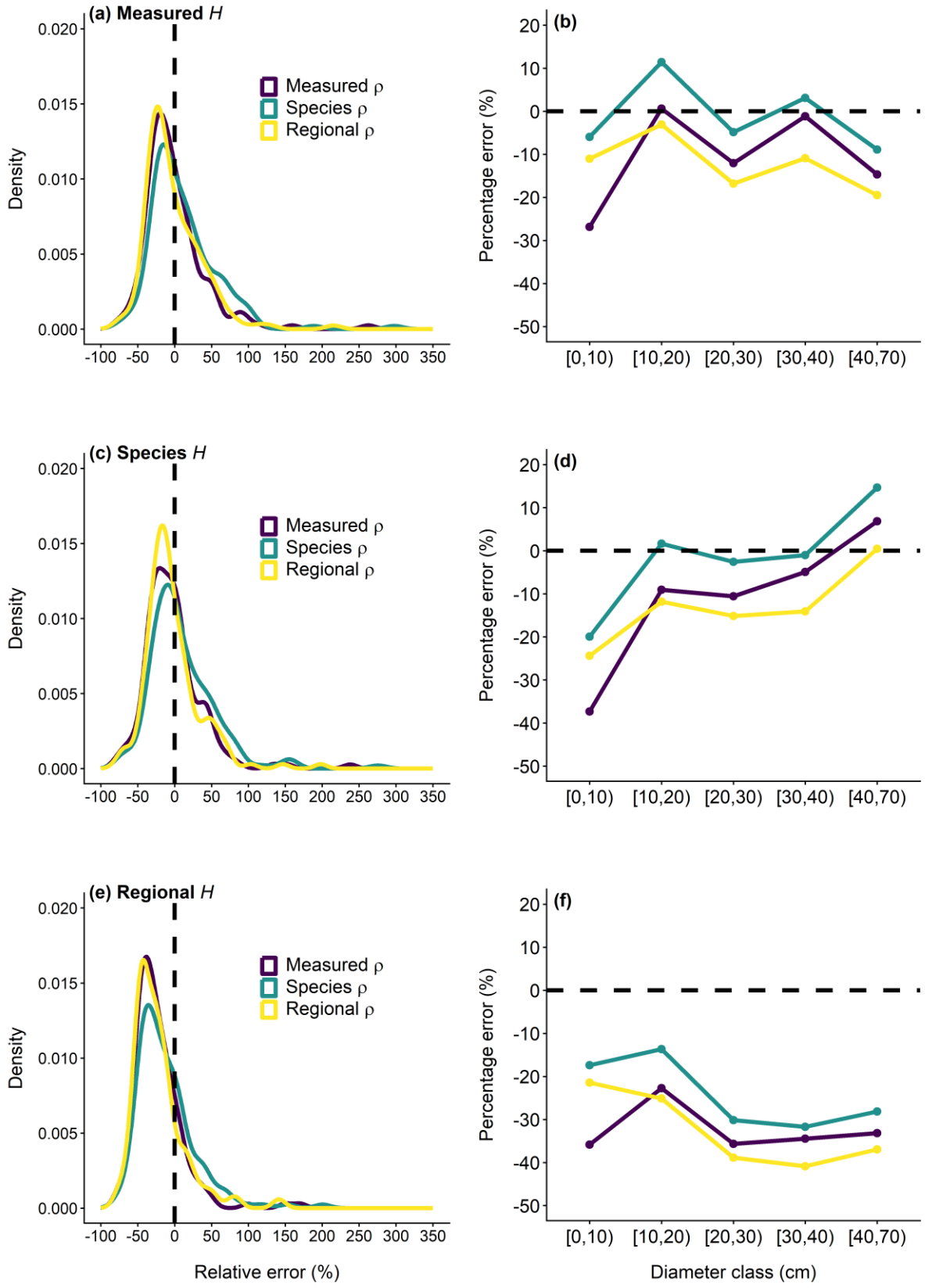


389

390 **Figure 4.** Errors in aboveground biomass (*AGB*) estimation arising from uncertainty in tree
391 height (*H*) and wood density (ρ). Each panel corresponds to one of the nine scenarios described
392 in Table 3 in which we altered inputs of *H* and ρ in the *AGB* model developed by Chave et al.
393 (2014). *H* inputs vary in uncertainty from left to right, from field measured, to those estimated
394 using a species-specific *H-D* model (eq. 7), and finally those derived from a regional *H-D*
395 model (eq. 8). ρ inputs vary in uncertainty from top to bottom, from field measured ρ values,
396 to species-specific (or closest taxonomic unit) mean values derived from the Global Wood
397 Density Database, and finally those based on a single regional mean value for African tropical

398 forests derived from the literature. The orange coloured solid lines correspond to the fit of a
399 linear model between observed and predicted *AGB* values, while dashed lines illustrate a 1:1
400 relationship. Fit statistics for each model are reported in the panels, including the intercept (a)
401 and slope (b) of the regression line (with 95% confidence intervals in brackets), as well as the
402 RMSE and PE. Refer to Fig. S8 for a similar plot but excluding the largest/observed *AGB* value
403 which , by visual inspection, appears like an outlier when compared to other data values.

404


(a) Measured H
(b)
(c) Species H
(d)
(e) Regional H
(f)
Measured ρ
Species ρ
Regional ρ
Density
Percentage error (%)
Relative error (%)
Diameter class (cm)
[0,10)
[10,20)
[20,30)
[30,40)
[40,70)

405

406

407 **Figure 5.** Errors in aboveground biomass (*AGB*) estimation due to uncertainty in tree height
408 (*H*) and wood density (ρ) across the nine scenarios depicted in Table 3. Panels on the left show
409 the distribution of relative errors, as a percentage, (calculated as: $((\widehat{AGB}_i - AGB_i)/AGB_i) \times$
410 100; where AGB_i is the measured AGB for tree i; and $\widehat{AGB}_i$ is the estimated AGB for tree i) in
411 *AGB* across the nine scenarios, while those on the right show the percentage error (PE, in %)
412 for trees grouped into the five stem diameter classes across scenarios. In all cases, *AGB* was
413 estimated using the pan-tropical model developed by Chave et al. (2014). Species *H* (Fig. 5c)
414 refers to using eq. 7 to estimate tree *H* while regional *H* (Fig. 5e) corresponds to using eq. 8 to
415 estimate tree *H*.

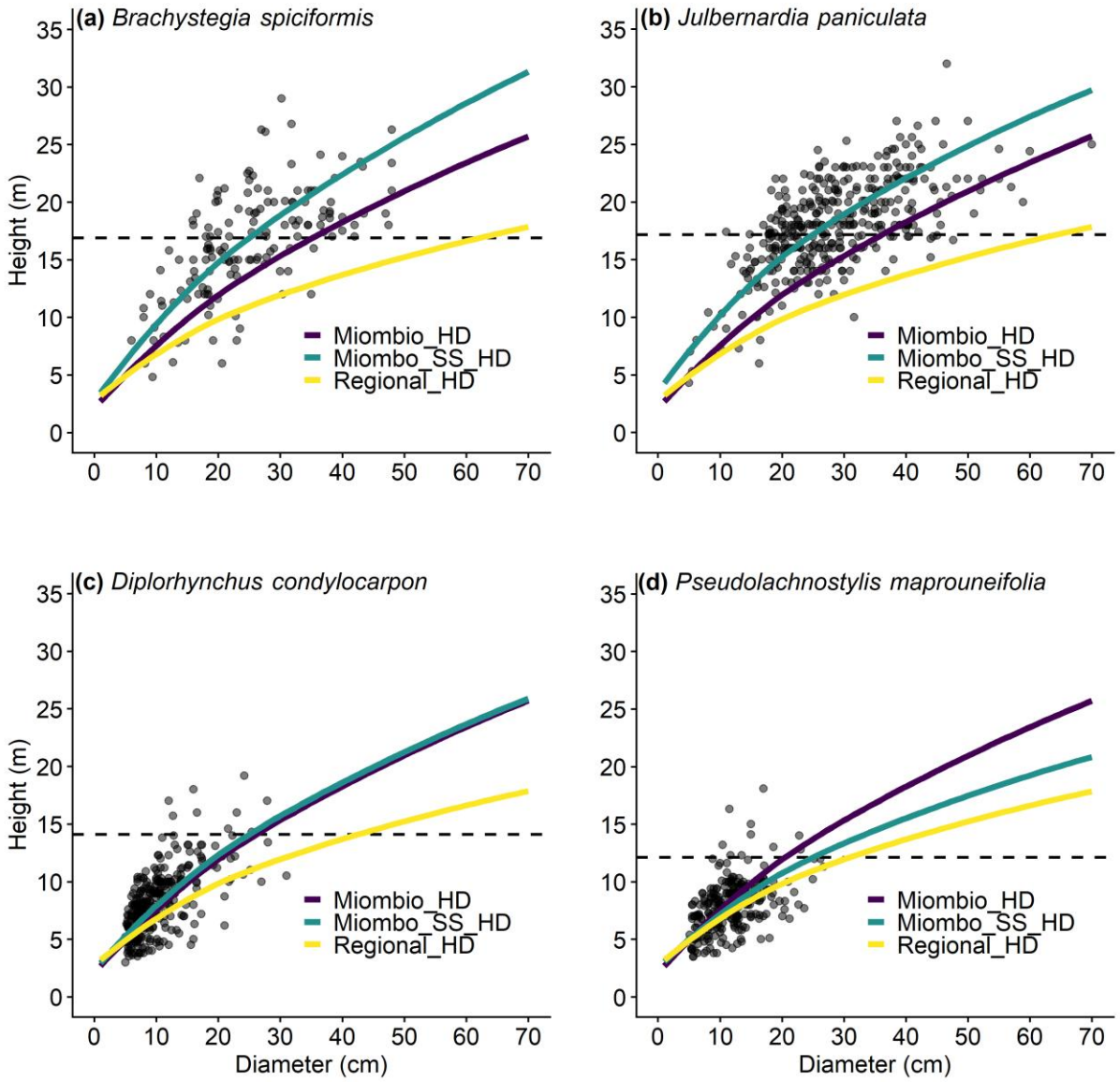


Figure 6. Variability in height-diameter (*H-D*) relationships among common miombo tree species with differing adult statures. Fitted lines correspond to the population-level fit of eq. 7(purple), the species-level deviations from the population-level fit (green; see Table S4 for species-level parameter values), and the fit of the regional *H-D* allometry derived from the Tallo database (yellow; eq. 8). The horizontal dashed black lines show the height prediction for a tree with diameter of 25 cm using the species-specific *H-D* model.

4. DISCUSSION

4.1 Strength in numbers: pantropical model provides robust estimates of *AGB*

Our study shows that when accurate measurements or estimates of tree height and wood density are available, the pantropical model developed by Chave et al. (2014) can generate unbiased estimates of *AGB*. In fact in our case, this pantropical model performed similarly well to *AGB* equations calibrated against new data (Fig. 3 and Fig. S4). A key feature of this pantropical model is that compared to other regional or species-specific models that exist in the literature, it was developed using a large number of harvested trees (>4000) that span a broad range of environments and sizes. This is clearly a major strength when it comes to making predictions against new data. A priority for future research in this field should therefore be to further consolidate and expand data on harvested trees into a common database so that robust and widely applicable *AGB* models can be built.

By contrast, we found that the regional ILUA2 model developed to predict *AGB* for Zambia's forests as part of the national forest inventory severely underestimated *AGB*, particularly that of large trees. There are two plausible reasons for this underestimation. First, although the ILUA2 model was developed using 1319 harvested trees, these comprised mostly small to medium size trees ($D \leq 30$cm) (Forestry Department, 2016). Small sample sizes and/or large sample sizes with mostly smaller trees to parameterize *AGB* models have been identified as major sources of *AGB* errors and uncertainty (Chave et al., 2004). Second, the ILUA2 model uses *D* as the sole predictor of *AGB*. While *D* is clearly the single strongest correlate of *AGB* (Fig. 1b), in doing so the model does not account for differences in *H-D* scaling among species (Fig. 6) and forest types (Timberlake et al., 2010; Munalula et al., 2020; Yambayamba et al., 2025), nor does it incorporate variability in wood density which can substantially affect *AGB* estimates (Mitchard et al., 2014; Jucker et al., 2018; Phillips et al., 2019). Our findings align with a recent study in the same region suggesting that commonly applied allometric models

underestimate *AGB* of miombo woodlands (Demol et al., 2024). This has important practical implications, including reporting and verification of forest carbon stocks and dynamics under REDD+ and emerging carbon trading initiatives (Köhl et al., 2020; GRZ, 2021; Melo et al., 2023), as well as the calibration and validation of satellite-derived estimates of forest carbon stocks. For instance, Zambia has previously used the ILUA2 model to estimate FREL submissions to the UNFCCC (GRZ, 2016) but most recently identified the pantropical model for consideration (GRZ, 2021). In this respect, our study highlights the challenges associated with accurate estimation of *AGB* stocks and therefore underscores the need for rigorous methods for quantifying *AGB* stocks and dynamics in miombo woodlands and beyond.

4.2 Tree height uncertainty can severely bias *AGB* estimates

Our study reiterates the recommendation of previous works to account for tree height when estimating *AGB* (Feldpausch et al., 2012; Chave et al., 2014; Djomo et al., 2016; Handavu et al., 2021). However, our results also underscore how the inclusion of *H* in *AGB* models is not without its challenges (Chave et al., 2014; Kapinga et al., 2018). First, conventional field measurements of *H* are not only time consuming to take but also prone to errors, especially for large trees and in closed canopies (Larjavaara and Muller-Landau, 2013; Wang et al., 2019). Second, the common practice of using *H-D* models to estimate tree height when this is not measured is equally subject to errors, especially where locally fitted *H-D* models are unavailable (Fayolle et al., 2016; Sullivan et al., 2018). In line with previous studies, our results demonstrate the peril of applying generic and regional *H-D* models to specific locations that are environmentally or taxonomically distinct (Feldpausch et al., 2012; Kearsley et al., 2013; Molto et al., 2014; Ledo et al., 2016; Fayolle et al., 2016). Using a regional *H-D* model developed for tropical dry forests led to a severe underestimation of *AGB*. Worse still, this underestimation increased with *D* (Fig. 5f), which is particularly undesirable since larger trees contribute disproportionately to total forest carbon stocks (Fig. 1a; (Lutz et al., 2018)). Our

approach of fitting a locally-calibrated and species-specific *H-D* model substantially improved the accuracy of *AGB* estimates. However, access to high-quality local datasets to parameterize such allometries is often limited (Jucker et al., 2022).

The importance of tree height in *AGB* estimation has also been demonstrated in studies using remote sensing methods to map forest structure. For example, detailed reconstructions of tree architecture made possible by terrestrial laser scanning have shown that traditional allometric models can underestimate tree height and therefore *AGB* (Calders et al., 2022; Terryn et al., 2024). Given the obvious challenges associated with accurate measurement of *H* using conventional field methods, we argue that improvement in *AGB* estimation in miombo woodlands requires leveraging increasingly available and affordable remote sensing technologies such as LiDAR (Momo Takoudjou et al., 2018; Calders et al., 2022; Demol et al., 2022; Demol et al., 2024). These data provide a robust way to characterise the 3D architecture of trees that can be used to describe forest structure, functioning and dynamics with greater accuracy and across larger scales than traditional field methods (Jucker et al., 2023; Battison et al., 2024).

4.3 The importance of accounting for wood density when estimating *AGB*

Wood density can vary considerably among tree species, with values ranging almost three fold from as low as 0.34 g cm^{-3} to 0.86 g cm^{-3} across those sampled in our study. As previous work in Amazonia has shown, failure to properly account for this variability in wood density among species and forest types can severely bias large-scale estimates of forest carbon stocks inferred via remote sensing (Mitchard et al., 2014; Phillips et al., 2019). In the case of the miombo woodlands studied here, uncertainty in wood density was of secondary importance to that in tree height in driving errors in *AGB* estimation. But this is likely to differ among forest types and will depend on both the accuracy of available *H–D* allometries and the coverage of wood density databases like the GWDD.

When field-measured values of wood density were replaced with ones obtained from the GWDD, we found that overall wood density was overestimated across the population. This led to only a modest reduction in underestimation of *AGB*, as wood density values from the GWDD were generally correlated to those measured in the field (Fig. S7). This confirms previous work showing that while wood density can vary somewhat within species, it is generally quite a conserved trait (Chave et al., 2009; Fischer et al., 2026). Therefore, provided trees have been identified to species level and that these species have matching observations in the GWDD, our results suggest that *AGB* can be estimated with limited bias. This provides a strong incentive to continue to curate and expand field reference collections of wood density to support large-scale mapping of forest carbon stocks (Fischer et al., 2026). In the context of Zambia's miombo woodlands, only 31 tree species (out of approximately 238 species identified in the most recent national forest inventory (Pelletier et al., 2018; Yambayamba et al., 2025)) have wood density records (Forestry Department, 2016), making it imperative that taxonomic coverage is increased in the future.

Uncertainty in wood density can compound the errors in *AGB* associated with the use of a generic *H–D* allometry, but it is easy to imagine a situation in which these errors could instead cancel each other out, making them even harder to detect and quantify. In this regard, our framework provides a simple and robust way to decompose errors in *AGB* arising from uncertainty in both height and wood density. Replicating this analysis on a larger dataset, such as the pantropical *AGB* database developed by Chave et al. (2014), would provide valuable insights into the main sources of error in *AGB* estimation and how these vary across forest types and biogeographic regions.

5. CONCLUSION

Our study aimed at comparing the predictive performance of existing and reparametrized *AGB* models in miombo woodlands and quantifying the errors associated with using different approaches to imputing of height and wood density. We have shown that using *AGB* models that incorporate *H* and ρ, in addition to *D*, provide better and more transferable estimates than those that rely exclusively on *D*. The reparametrized model of Chavel et al. (2014) we develop here thus provides a good starting point for improving *AGB* estimates in miombo woodlands. However, looking ahead, we encourage the research community to continue to move towards larger, integrated databases of tree *AGB* in order to develop generalised models that can underpin accurate accounting of forest carbon stocks under REDD+ and carbon trading initiatives.

Our study further revealed that uncertainty in *H* (more than in ρ in the miombo) can lead to substantial errors in *AGB* estimates. Since *H* is typically only measured for a small sub-sample of trees and mostly estimated using *H-D* models in conventional forest inventories, we therefore reiterate that great care is needed when selecting the approach to estimate *H* (particularly if locally available *H* data are not available to assess model performance). Collating and curating accurately measured *H-D* data and developing local species-specific *H-D* allometries remain a priority for the miombo and many other regions (particularly those in the tropics). The species-specific *H-D* models we develop here thus serve as a baseline for improving *AGB* estimation in miombo woodlands, although future work should also consider comparing different functional forms for modelling *H-D* relationships (Cano et al., 2019).

The *AGB* and *H-D* allometries developed in this study will hopefully serve as a blueprint for improving the characterization and modelling of tree allometry, ecosystem function and biomass estimation in miombo woodlands. In particular, emerging remote sensing technologies such as terrestrial and airborne LiDAR are increasingly being used to characterize

545 tree structure and map landscape-scale carbon stocks, but require field based approaches for
546 validation and calibration (Jucker et al., 2017; Chave et al., 2019). Similarly, improved
547 allometries are crucial to accurate simulation of vegetation response to environmental change
548 in dynamic global vegetation models (Fischer et al., 2019).

549

ACKNOWLEDGEMENTS

Arthur M. Yambayamba (AMY) was supported by a PhD scholarship through the Commonwealth Scholarship Commission (CSC) programme (grant: ZMCS-2021-542). Tommaso Jucker (TJ) was supported by a NERC Independent Research Fellowship (grant: NE/S01537X/1) and through a UKRI Frontier Research grant (grant: EP/Y003810/1) that also supported AMY.

AUTHOR CONTRIBUTIONS

AMY and TJ designed the study. Kondwani Kapinga (KK) did the vegetation assessment, forest inventory, destructive sampling and laboratory analysis for the Mwekera forest dataset. Ferdinand Handavu (FH) did the vegetation assessment, forest inventory, destructive sampling and laboratory analysis, with assistance from KK, for the Katanino and Miengwe forests datasets. AMY did the data collating and led the analysis with assistance from TJ. AMY wrote the first draft of the manuscript with all the authors contributing substantially to revisions.

CONFLICT OF INTEREST

The authors declare no competing interests.

DATA AND CODE AVAILABILITY STATEMENT

Data and R code to replicate the results of this study will be publicly archived on Zenodo following the review of this paper.

SUPPLEMENTARY MATERIAL

Additional supporting information may be found online in the Supporting Information section.

REFERENCES

Aphalo, P.: _ggpmisc: Miscellaneous Extensions to 'ggplot2'_. R package version 0.6.0,, <https://CRAN.R-project.org/package=ggpmisc>. 2024.

Arias, P. A., N. Bellouin, E. Coppola, R.G. Jones, G. Krinner, J. Marotzke, V. Naik, M.D. Palmer, G.-K. Plattner, J.Rogelj, M. Rojas, J. Sillmann, T. Storelvmo, P.W. Thorne, B. Trewin, K. Achuta Rao, B. Adhikary, R.P. Allan, K.Armour, G. Bala, R. Barimalala, S. Berger, J.G. Canadell, C. Cassou, A. Cherchi, W. Collins, W.D. Collins, S.L. Connors, S. Corti, F. Cruz, F.J. Dentener, C. Dereczynski, A. Di Luca, A. Diongue Niang, F.J. Doblas-Reyes, A. Dosio, H. Douville, F. Engelbrecht, V. Eyring, E. Fischer, P. Forster, B. Fox-Kemper, J.S. Fuglestvedt, J.C. Fyfe, N.P. Gillett, L. Goldfarb, I. Gorodetskaya, J.M. Gutierrez, R. Hamdi, E. Hawkins, H.T. Hewitt, P. Hope, A.S. Islam, C. Jones, D.S. Kaufman, R.E. Kopp, Y. Kosaka, J. Kossin, S. Krakovska, J.-Y. Lee, J. Li, T. Mauritsen, T.K. Maycock, M. Meinshausen, S.-K. Min, P.M.S. Monteiro, T. Ngo-Duc, F. Otto, I. Pinto, A. Pirani, K. Raghavan, R. Ranasinghe, A.C. Ruane, L. Ruiz, J.-B. Sallée, B.H. Samset, S. Sathyendranath, S.I. Seneviratne, A.A. Sörensson, S. Szopa, I. Takayabu, A.-M. Tréguier, B. van den Hurk, R. Vautard, K. von Schuckmann, S. Zaehle, X. Zhang, and K. Zickfeld: Climate Change 2021: The Physical Science Basis. Contribution of Working Group I to the Sixth Assessment Report of the Intergovernmental Panel on Climate Change; Technical Summary, in, edited by: Masson-Delmotte, V., P. Zhai, A. Pirani, S.L. Connors, C. Péan, S. Berger, N. Caud, Y. Chen, L. Goldfarb, M.I. Gomis, M. Huang, K. Leitzell, E. Lonnoy, J.B.R., Matthews, T.K. Maycock, T. Waterfield, O. Yelekçi, R. Yu, and Zhou, B., Cambridge University Press, Cambridge, United Kingdom and New York, NY, USA , pp. 33−144, doi:10.1017/9781009157896.002., 33-144, 10.1017/9781009157896.002, 2021.

Banin, L., Feldpausch, T. R., Phillips, O. L., Baker, T. R., Lloyd, J., Affum-Baffoe, K., Arets, E., Berry, N. J., Bradford, M., and Brienen, R. J. W.: What controls tropical forest architecture? Testing environmental, structural and floristic drivers, Global Ecology and Biogeography, 21, 1179-1190, 2012.

Baskerville, G.: Use of logarithmic regression in the estimation of plant biomass, Canadian Journal of Forest Research, 2, 49-53, 1972.

599 Battison, R., Prober, S. M., Zdunic, K., Jackson, T. D., Fischer, F. J., and Jucker, T.: Tracking
600 tree demography and forest dynamics at scale using remote sensing, New Phytologist, 244,
601 2251-2266, 2024.

602 Bomfim, B., Pinagé, E. R., Emmert, F., and Kueppers, L. M.: Improving sustainable tropical
603 forest management with voluntary carbon markets, Plant and Soil, 1-8, 2022.

604 Brown, M. J. M., Walker, B. E., Black, N., Govaerts, R. H. A., Ondo, I., Turner, R., and Nic
605 Lughadha, E.: rWCVP: a companion R package for the World Checklist of Vascular Plants,
606 New Phytologist, 240, 1355-1365, https://doi.org/10.1111/nph.18919, 2023.

607 Brun, P., Zimmermann, N. E., Hari, C., Pellissier, L., and Karger, D. N.: Global climate-related
608 predictors at kilometre resolution for the past and future, Earth Syst. Sci. Data Discuss., 2022,
609 1-44, 10.5194/essd-2022-212, 2022.

610 Bürkner, P.-C.: brms: An R Package for Bayesian Multilevel Models Using Stan, Journal of
611 Statistical Software, 80, 1 - 28, 10.18637/jss.v080.i01, 2017.

612 Calders, K., Verbeeck, H., Burt, A., Origo, N., Nightingale, J., Malhi, Y., Wilkes, P., Raumonen,
613 P., Bunce, R. G. H., and Disney, M.: Laser scanning reveals potential underestimation of
614 biomass carbon in temperate forest, Ecological Solutions and Evidence, 3, e12197,
615 https://doi.org/10.1002/2688-8319.12197, 2022.

616 Cano, M. I., Muller-Landau, H. C., Wright, S. J., Bohlman, S. A., and Pacala, S. W.: Tropical
617 tree height and crown allometries for the Barro Colorado Nature Monument, Panama: a
618 comparison of alternative hierarchical models incorporating interspecific variation in relation
619 to life history traits, Biogeosciences, 16, 847-862, 2019.

620 Chamshama, S., Mugasha, A., and Zahabu, E.: Stand biomass and volume estimation for
621 Miombo woodlands at Kitulangalo, Morogoro, Tanzania, The Southern African Forestry
622 Journal, 200, 59-70, 2004.

623 Chave, J., Condit, R., Aguilar, S., Hernandez, A., Lao, S., and Perez, R.: Error propagation and
624 scaling for tropical forest biomass estimates, Philosophical Transactions of the Royal Society
625 of London. Series B: Biological Sciences, 359, 409-420, 2004.

626 Chave, J., Coomes, D., Jansen, S., Lewis, S. L., Swenson, N. G., and Zanne, A. E.: Towards a
627 worldwide wood economics spectrum, Ecology letters, 12, 351-366, 2009.

628 Chave, J., Davies, S. J., Phillips, O. L., Lewis, S. L., Sist, P., Schepaschenko, D., Armston, J.,
629 Baker, T. R., Coomes, D., and Disney, M.: Ground data are essential for biomass remote sensing
630 missions, Surveys in Geophysics, 1-18, 2019.

631 Chave, J., Réjou-Méchain, M., Búrquez, A., Chidumayo, E., Colgan, M. S., Delitti, W. B. C.,
632 Duque, A., Eid, T., Fearnside, P. M., and Goodman, R. C.: Improved allometric models to
633 estimate the aboveground biomass of tropical trees, Global change biology, 20, 3177-3190,
634 2014.

635 Chidumayo, E.: Development of Brachystegia-Julbernardia woodland after clear-felling in
636 central Zambia: Evidence for high resilience, Applied Vegetation Science, 7, 237-242, 2004.

637 Chidumayo, E. N.: Forest degradation and recovery in a miombo woodland landscape in
638 Zambia: 22 years of observations on permanent sample plots, Forest Ecology and Management,
639 291, 154-161, 2013a.

640 Chidumayo, E. N.: Estimating tree biomass and changes in root biomass following clear-
641 cutting of Brachystegia-Julbernardia (miombo) woodland in central Zambia, Environmental
642 conservation, 41, 54-63, 2013b.

643 Chojnacky, D. C., Heath, L. S., and Jenkins, J. C.: Updated generalized biomass equations for
644 North American tree species, Forestry, 87, 129-151, 2014.

645 Clark, D. B. and Kellner, J. R.: Tropical forest biomass estimation and the fallacy of misplaced
646 concreteness, Journal of Vegetation Science, 23, 1191-1196, 2012.

647 Colgan, M. S., Asner, G. P., and Swemmer, T.: Harvesting tree biomass at the stand level to
648 assess the accuracy of field and airborne biomass estimation in savannas, Ecological
649 Applications, 23, 1170-1184, https://doi.org/10.1890/12-0922.1, 2013.

650 Demol, M., Verbeeck, H., Gielen, B., Armston, J., Burt, A., Disney, M., Duncanson, L.,
651 Hackenberg, J., Kükenbrink, D., and Lau, A.: Estimating forest above-ground biomass with
652 terrestrial laser scanning: Current status and future directions, Methods in Ecology and
653 Evolution, 13, 1628-1639, 2022.

654 Demol, M., Aguilar-Amuchastegui, N., Bernotaite, G., Disney, M., Duncanson, L., Elmendorp,
655 E., Espejo, A., Furey, A., Hancock, S., Hansen, J., Horsley, H., Langa, S., Liang, M., Locke,
656 A., Manjate, V., Mapanga, F., Omidvar, H., Parsons, A., Peneva-Reed, E., Perry, T., Puma Vilca,
657 B. L., Rodríguez-Veiga, P., Sutcliffe, C., Upham, R., de Walque, B., and Burt, A.: Multi-scale

lidar measurements suggest miombo woodlands contain substantially more carbon than thought, Communications Earth & Environment, 5, 366, 10.1038/s43247-024-01448-x, 2024.

Djomo, A. N., Picard, N., Fayolle, A., Henry, M., Ngomanda, A., Ploton, P., McLellan, J., Saborowski, J., Adamou, I., and Lejeune, P.: Tree allometry for estimation of carbon stocks in African tropical forests, Forestry: An International Journal of Forest Research, 89, 446-455, 2016.

Dowle, M. and Srinivasan, A.: _data.table: Extension of `data.frame`_ R package version 1.14.8, <https://CRAN.R-project.org/package=data.table>, 2023.

Dubayah, R., Blair, J. B., Goetz, S., Fatoyinbo, L., Hansen, M., Healey, S., Hofton, M., Hurtt, G., Kellner, J., Luthcke, S., Armston, J., Tang, H., Duncanson, L., Hancock, S., Jantz, P., Marselis, S., Patterson, P. L., Qi, W., and Silva, C.: The Global Ecosystem Dynamics Investigation: High-resolution laser ranging of the Earth's forests and topography, Science of Remote Sensing, 1, 100002, https://doi.org/10.1016/j.srs.2020.100002, 2020.

Dziba, L., Ramoelo, A., Ryan, C., Harrison, S., Pritchard, R., Tripathi, H., Sitas, N., Selomane, O., Engelbrecht, F., Pereira, L., Katerere, Y., Chirwa, P. W., Ribeiro, N. S., and Grundy, I. M.: Scenarios for Just and Sustainable Futures in the Miombo Woodlands, in: Miombo Woodlands in a Changing Environment: Securing the Resilience and Sustainability of People and Woodlands, edited by: Ribeiro, N. S., Katerere, Y., Chirwa, P. W., and Grundy, I. M., Springer International Publishing, Cham, 191-234, 10.1007/978-3-030-50104-4_6, 2020.

Ellis, E. C., Gauthier, N., Klein Goldewijk, K., Bliege Bird, R., Boivin, N., Díaz, S., Fuller, D. Q., Gill, J. L., Kaplan, J. O., Kingston, N., Locke, H., McMichael, C. N. H., Ranco, D., Rick, T. C., Shaw, M. R., Stephens, L., Svenning, J.-C., and Watson, J. E. M.: People have shaped most of terrestrial nature for at least 12,000 years, Proceedings of the National Academy of Sciences, 118, e2023483118, doi:10.1073/pnas.2023483118, 2021.

Fareed, N. and Numata, I.: Evaluating the impact of field-measured tree height errors correction on aboveground biomass modeling using airborne laser scanning and GEDI datasets in Brazilian Amazonia, Trees, Forests and People, 100751, https://doi.org/10.1016/j.tfp.2024.100751, 2024.

Fayolle, A., Panzou, G. J. L., Drouet, T., Swaine, M. D., Bauwens, S., Vleminckx, J., Biwole, A., Lejeune, P., and Doucet, J.-L.: Taller trees, denser stands and greater biomass in semi-

deciduous than in evergreen lowland central African forests, Forest Ecology and Management, 374, 42-50, 2016.

Feldpausch, T. R., Banin, L., Phillips, O. L., Baker, T. R., Lewis, S. L., Quesada, C. A., Affum-Baffoe, K., Arets, E. J. M. M., Berry, N. J., and Bird, M.: Height-diameter allometry of tropical forest trees, Biogeosciences, 2011.

Feldpausch, T. R., Lloyd, J., Lewis, S. L., Brienen, R. J., Gloor, M., Monteagudo Mendoza, A., Lopez-Gonzalez, G., Banin, L., Abu Salim, K., and Affum-Baffoe, K.: Tree height integrated into pantropical forest biomass estimates, Biogeosciences, 3381-3403, 2012.

Fischer, F. J., Maréchaux, I., and Chave, J.: Improving plant allometry by fusing forest models and remote sensing, New Phytologist, 223, 1159-1165, 2019.

Fischer, F. J., Chave, J., Zanne, A., Jucker, T., Fajardo, A., Fayolle, A., de Lima, R. A. F., Vieilledent, G., Beeckman, H., Hubau, W., De Mil, T., Wallenus, D., Aldana, A. M., Alvarez-Dávila, E., Alves, L. F., Apgaua, D. M. G., Arcanjo, F., Bastin, J.-F., Bilous, A., Birnbaum, P., Blyshchyk, V., Borah, J., Boukili, V., Camarero, J. J., Casas, L., Cazzolla Gatti, R., Chambers, J. Q., Fabiano, E. C., Choat, B., Conti, G., Cornwell, W., Dar, J. A., Das, A. K., Dobler, M., Dougabka, D., Edwards, D. P., Evans, R., Falster, D., Fearnside, P., Flores, O., Fyllas, N., Gérard, J., Goodman, R. C., Guibal, D., Henao-Diaz, L. F., Hervé, V., Hietz, P., Homeier, J., Ibanez, T., Ilic, J., Jansen, S., Kalita, R. M., Kenzo, T., Kindermann, L., Kothandaraman, S., Kotowska, M., Kubota, Y., Langbour, P., Lawson, J., de Lima, A. L. A., Link, R. M., Linstädter, A., López, R., Macinnis-Ng, C., Magnago, L. F. S., Martin, A. R., Matheny, A. M., McCarthy, J. K., Miller, R. B., Nath, A. J., Nelson, B. W., Njana, M., Nogueira, E. M., Oliveira, A., Oliveira, R., Olson, M., Onoda, Y., Paul, K., Piotto, D., Radtke, P., Razafindratsima, O., Ramananantoandro, T., Read, J., Richardson, S., de la Riva, E. G., Rodríguez-Reyes, O., Rolim, S. G., Rolo, V., Rosell, J. A., Salguero-Gómez, R., Santini, N. S., Schuldt, B., Schwendenmann, L., Sellin, A., Staples, T., Stevenson, P. R., Sundarapandian, S., van der Sande, M. T., Thibaut, B., Tng, D. Y. P., Torezan, J. M. D., Villanueva, B., Weiskittel, A., Wells, J., Wright, S. J., and Zieminska, K.: Beyond species means – the intraspecific contribution to global wood density variation, New Phytologist, n/a, https://doi.org/10.1111/nph.70860, 2026.

Flores, O. and Coomes, D. A.: Estimating the wood density of species for carbon stock assessments, Methods in Ecology and Evolution, 2, 214-220, 2011.

718 Forestry Department: Ministry of Lands Natural Resources and Environmental Protection,
719 Integrated Land Use Assessment Phase II - Technical Paper 3, *Assessment of Existing Models*
720 *for Biomass Volume Calculations*. Food and Agricultural Organization of the United Nations,
721 Ministry of Foreign Affairs Finland. Lusaka, Zambia., 59, 2016.

722 Goodman, R. C., Phillips, O. L., and Baker, T. R.: The importance of crown dimensions to
723 improve tropical tree biomass estimates, Ecological Applications, 24, 680-698, 2014.

724 Govaerts, R., Nic Lughadha, E., Black, N., Turner, R., and Paton, A.: The World Checklist of
725 Vascular Plants, a continuously updated resource for exploring global plant diversity, Scientific
726 Data, 8, 215, 10.1038/s41597-021-00997-6, 2021.

727 Grantham, H. S., Duncan, A., Evans, T. D., Jones, K. R., Beyer, H. L., Schuster, R., Walston,
728 J., Ray, J. C., Robinson, J. G., Callow, M., Clements, T., Costa, H. M., DeGemmis, A., Elsen,
729 P. R., Ervin, J., Franco, P., Goldman, E., Goetz, S., Hansen, A., Hofsvang, E., Jantz, P., Jupiter,
730 S., Kang, A., Langhammer, P., Laurance, W. F., Lieberman, S., Linkie, M., Malhi, Y., Maxwell,
731 S., Mendez, M., Mittermeier, R., Murray, N. J., Possingham, H., Radachowsky, J., Saatchi, S.,
732 Samper, C., Silverman, J., Shapiro, A., Strassburg, B., Stevens, T., Stokes, E., Taylor, R., Tear,
733 T., Tizard, R., Venter, O., Visconti, P., Wang, S., and Watson, J. E. M.: Anthropogenic
734 modification of forests means only 40% of remaining forests have high ecosystem integrity,
735 Nature Communications, 11, 5978, 10.1038/s41467-020-19493-3, 2020.

736 GRZ: Zambia's Forest Reference Emissions Level Submission to the UNFCCC, 41,
737 https://redd.unfccc.int/files/2016_submission_frel_zambia.pdf Date Accessed: 20/12/2021,
738 2016.

739 GRZ: Zambia's Forest Reference Emissions Level Submission to the UNFCCC, 41,
740 https://redd.unfccc.int/files/zambia_frel-2020-technical_assessment.pdf Date Accessed:
741 20/01/2022, 2021.

742 Guedes, B. S., Sitoe, A. A., and Olsson, B. A.: Allometric models for managing lowland
743 miombo woodlands of the Beira corridor in Mozambique, Global ecology and conservation,
744 13, e00374, 2018.

745 Handavu, F., Syampungani, S., Sileshi, G. W., and Chirwa, P. W.: Aboveground and
746 belowground tree biomass and carbon stocks in the miombo woodlands of the Copperbelt in
747 Zambia, Carbon Management, 1-15, 2021.

748 Henry, M., Bombelli, A., Trotta, C., Alessandrini, A., Birigazzi, L., Sola, G., Vieilledent, G.,
749 Santenoise, P., Longuetaud, F., Valentini, R., Picard, N., and Saint-André, L.: GlobAllomeTree:
750 international platform for tree allometric equations to support volume, biomass and carbon
751 assessment, iForest - Biogeosciences and Forestry, 6, 326-330, 10.3832/ifor0901-006, 2013.

752 Hijmans, R.: _terra: Spatial Data Analysis_. R package version 1.7-39,, <https://CRAN.R-
753 project.org/package=terra>. 2023.

754 Hua, F., Liu, M., and Wang, Z.: Integrating forest restoration into land-use planning
755 at large spatial scales, Current Biology, 34, R452-R472, 10.1016/j.cub.2024.02.034,
756 2024.

757 ILUA: Integrated land use assessment phase II–report for Zambia, The Food and Agriculture
758 Organization of the United Nations and the Forestry Department, Ministry of Lands and
759 Natural Resources, Lusaka, Zambia, www. zmb-nfms. org/iluaii/index. php, 2016.

760 Jucker, T., Bongalov, B., Burslem, D. F. R. P., Nilus, R., Dalponte, M., Lewis, S. L., Phillips,
761 O. L., Qie, L., and Coomes, D. A.: Topography shapes the structure, composition and function
762 of tropical forest landscapes, Ecology Letters, 21, 989-1000, https://doi.org/10.1111/ele.12964,
763 2018.

764 Jucker, T., Caspersen, J., Chave, J., Antin, C., Barbier, N., Bongers, F., Dalponte, M., van
765 Ewijk, K. Y., Forrester, D. I., and Haeni, M.: Allometric equations for integrating remote
766 sensing imagery into forest monitoring programmes, Global change biology, 23, 177-190,
767 2017.

768 Jucker, T., Gosper, C. R., Wiehl, G., Yeoh, P. B., Raisbeck-Brown, N., Fischer, F. J., Graham,
769 J., Langley, H., Newchurch, W., O'Donnell, A. J., Page, G. F. M., Zdunic, K., and Prober, S.
770 M.: Using multi-platform LiDAR to guide the conservation of the world's largest temperate
771 woodland, Remote Sensing of Environment, 296, 113745,
772 https://doi.org/10.1016/j.rse.2023.113745, 2023.

773 Jucker, T., Fischer, F. J., Chave, J., Coomes, D. A., Caspersen, J., Ali, A., Loubota Panzou, G.
774 J., Feldpausch, T. R., Falster, D., Usoltsev, V. A., Adu-Bredu, S., Alves, L. F., Aminpour, M.,
775 Angoboy, I. B., Anten, N. P. R., Antin, C., Askari, Y., Muñoz, R., Ayyappan, N., Balvanera, P.,
776 Banin, L., Barbier, N., Battles, J. J., Beeckman, H., Bocko, Y. E., Bond-Lamberty, B., Bongers,
777 F., Bowers, S., Brade, T., van Breugel, M., Chantrain, A., Chaudhary, R., Dai, J., Dalponte, M.,
778 Dimobe, K., Domec, J.-C., Doucet, J.-L., Duursma, R. A., Enríquez, M., van Ewijk, K. Y.,

779 Farfán-Rios, W., Fayolle, A., Forni, E., Forrester, D. I., Gilani, H., Godlee, J. L., Gourlet-
780 Fleury, S., Haeni, M., Hall, J. S., He, J.-K., Hemp, A., Hernández-Stefanoni, J. L., Higgins, S.
781 I., Holdaway, R. J., Hussain, K., Hutley, L. B., Ichie, T., Iida, Y., Jiang, H.-s., Joshi, P. R.,
782 Kaboli, H., Larsary, M. K., Kenzo, T., Kloeppel, B. D., Kohyama, T., Kunwar, S., Kuyah, S.,
783 Kvasnica, J., Lin, S., Lines, E. R., Liu, H., Lorimer, C., Loumeto, J.-J., Malhi, Y., Marshall, P.
784 L., Mattsson, E., Matula, R., Meave, J. A., Mensah, S., Mi, X., Momo, S., Moncrieff, G. R.,
785 Mora, F., Nissanka, S. P., O'Hara, K. L., Pearce, S., Pelissier, R., Peri, P. L., Ploton, P., Poorter,
786 L., Pour, M. J., Pourbabaei, H., Dupuy-Rada, J. M., Ribeiro, S. C., Ryan, C., Sanaei, A., Sanger,
787 J., Schlund, M., Sellan, G., Shenkin, A., Sonké, B., Sterck, F. J., Svátek, M., Takagi, K.,
788 Trugman, A. T., Ullah, F., Vadeboncoeur, M. A., Valipour, A., Vanderwel, M. C., Vovides, A.
789 G., Wang, W., Wang, L.-Q., Wirth, C., Woods, M., Xiang, W., Ximenes, F. d. A., Xu, Y.,
790 Yamada, T., and Zavala, M. A.: Tallo: A global tree allometry and crown architecture database,
791 Global Change Biology, 28, 5254-5268, https://doi.org/10.1111/gcb.16302, 2022.

792 Jucker, T., Fischer, F. J., Chave, J., Coomes, D. A., Caspersen, J., Ali, A., Loubota Panzou, G.
793 J., Feldpausch, T. R., Falster, D., Usoltsev, V. A., Jackson, T. D., Adu-Bredu, S., Alves, L. F.,
794 Aminpour, M., Angoboy Ilondea, B., Anten, N. P. R., Antin, C., Askari, Y., Ayyappan, N.,
795 Banin, L. F., Barbier, N., Battles, J. J., Beeckman, H., Bocko, Y. E., Bond-Lamberty, B.,
796 Bongers, F., Bowers, S., van Breugel, M., Chantrain, A., Chaudhary, R., Dai, J., Dalponte, M.,
797 Dimobe, K., Domec, J.-C., Doucet, J.-L., Dupuy Rada, J. M., Duursma, R. A., Enríquez, M.,
798 van Ewijk, K. Y., Farfán-Rios, W., Fayolle, A., Ferretti, M., Forni, E., Forrester, D. I., Gilani,
799 H., Godlee, J. L., Haeni, M., Hall, J. S., He, J.-K., Hemp, A., Hernández-Stefanoni, J. L.,
800 Higgins, S. I., Holdaway, R. J., Hussain, K., Hutley, L. B., Ichie, T., Iida, Y., Jiang, H.-S., Joshi,
801 P. R., Kaboli, H., Kazempour Larsary, M., Kenzo, T., Kloeppel, B. D., Kohyama, T. S., Kunwar,
802 S., Kuyah, S., Kvasnica, J., Lin, S., Lines, E. R., Liu, H., Lorimer, C., Loumeto, J.-J., Malhi,
803 Y., Marshall, P. L., Mattsson, E., Matula, R., Meave, J. A., Mensah, S., Mi, X., Momo, S. T.,
804 Moncrieff, G. R., Mora, F., Muñoz, R., Nissanka, S. P., Nur Hajar, Z. S., O'Hara, K. L., Pearce,
805 S., Pelissier, R., Peri, P. L., Ploton, P., Poorter, L., Pour, M. J., Pourbabaei, H., Ribeiro, S. C.,
806 Ryan, C., Sanaei, A., Sanger, J., Schlund, M., Sellan, G., Shenkin, A., Sonké, B., Sterck, F. J.,
807 Svátek, M., Takagi, K., Trugman, A. T., Vadeboncoeur, M. A., Valipour, A., Vanderwel, M. C.,
808 Vovides, A. G., Waldner, P., Wang, W., Wang, L.-Q., Wirth, C., Woods, M., Xiang, W., de
809 Aquino Ximenes, F., Xu, Y., Yamada, T., Zavala, M. A., and Zimmermann, N. E.: The global
810 spectrum of tree crown architecture, Nature Communications, 16, 4876, 10.1038/s41467-025-
811 60262-x, 2025.

Kachamba, D., Eid, T., and Gobakken, T.: Above-and belowground biomass models for trees in the miombo woodlands of Malawi, Forests, 7, 38, 2016.

Kanja, K., Zhang, C., and Atkinson, P. M.: Evaluating multi-seasonal SAR and optical imagery for above-ground biomass estimation using the national forest inventory of Zambia, International Journal of Applied Earth Observation and Geoinformation, 139, 104494, https://doi.org/10.1016/j.jag.2025.104494, 2025.

Kapinga, K., Syampungani, S., Kasubika, R., Yambayamba, A. M., and Shamaoma, H.: Species-specific allometric models for estimation of the above-ground carbon stock in miombo woodlands of Copperbelt Province of Zambia, Forest ecology and management, 417, 184-196, 2018.

Kearsley, E., De Haulleville, T., Hufkens, K., Kidimbu, A., Toirambe, B., Baert, G., Huygens, D., Kebede, Y., Defourny, P., and Bogaert, J.: Conventional tree height–diameter relationships significantly overestimate aboveground carbon stocks in the Central Congo Basin, Nature communications, 4, 2269, 2013.

Köhl, M., Neupane, P. R., and Mundhenk, P.: REDD+ measurement, reporting and verification – A cost trap? Implications for financing REDD+MRV costs by result-based payments, Ecological Economics, 168, 106513, https://doi.org/10.1016/j.ecolecon.2019.106513, 2020.

Kuyah, S., Sileshi, G. W., and Rosenstock, T. S.: Allometric models based on bayesian frameworks give better estimates of aboveground biomass in the miombo woodlands, Forests, 7, 13, 2016.

Larjavaara, M. and Muller-Landau, H. C.: Measuring tree height: a quantitative comparison of two common field methods in a moist tropical forest, Methods in Ecology and Evolution, 4, 793-801, 2013.

Ledo, A., Cornulier, T., Illian, J. B., Iida, Y., Kassim, A. R., and Burslem, D. F.: Re-evaluation of individual diameter: height allometric models to improve biomass estimation of tropical trees, Ecological Applications, 26, 2376-2382, 2016.

Lewis, S. L., Wheeler, C. E., Mitchard, E. T., and Koch, A.: Restoring natural forests is the best way to remove atmospheric carbon, Nature, 568, 25-28, 2019.

Lutz, J. A., Furniss, T. J., Johnson, D. J., Davies, S. J., Allen, D., Alonso, A., Anderson-Teixeira, K. J., Andrade, A., Baltzer, J., and Becker, K. M.: Global importance of large-diameter trees, Global Ecology and Biogeography, 27, 849-864, 2018.

McNicol, I. M., Ryan, C. M., and Mitchard, E. T.: Carbon losses from deforestation and widespread degradation offset by extensive growth in African woodlands, Nature communications, 9, 3045, 2018.

McNicol, I. M., Ryan, C. M., and Williams, M.: How resilient are African woodlands to disturbance from shifting cultivation?, Ecological Applications, 25, 2320-2336, https://doi.org/10.1890/14-2165.1, 2015.

Melo, J., Baker, T., Nemitz, D., Quegan, S., and Ziv, G.: Satellite-based global maps are rarely used in forest reference levels submitted to the UNFCCC, Environmental Research Letters, 18, 034021, 10.1088/1748-9326/acba31, 2023.

Mitchard, E. T., Feldpausch, T. R., Brienen, R. J., Lopez-Gonzalez, G., Monteagudo, A., Baker, T. R., Lewis, S. L., Lloyd, J., Quesada, C. A., and Gloor, M.: Markedly divergent estimates of A mazon forest carbon density from ground plots and satellites, Global Ecology and Biogeography, 23, 935-946, 2014.

Molto, Q., Hérault, B., Boreux, J.-J., Daullet, M., Rousteau, A., and Rossi, V.: Predicting tree heights for biomass estimates in tropical forests–a test from French Guiana, Biogeosciences, 11, 3121-3130, 2014.

Momo Takoudjou, S., Ploton, P., Sonké, B., Hackenberg, J., Griffon, S., de Coligny, F., Kamdem, N. G., Libalah, M., Mofack, G. I., Le Moguédec, G., Pélissier, R., and Barbier, N.: Using terrestrial laser scanning data to estimate large tropical trees biomass and calibrate allometric models: A comparison with traditional destructive approach, Methods in Ecology and Evolution, 9, 905-916, https://doi.org/10.1111/2041-210X.12933, 2018.

Mugasha, W. A., Eid, T., Bollandsås, O. M., Malimbwi, R. E., Chamshama, S. A. O., Zahabu, E., and Katani, J. Z.: Allometric models for prediction of above-and belowground biomass of trees in the miombo woodlands of Tanzania, Forest Ecology and Management, 310, 87-101, 2013.

Munalula, F., Seifert, T., and Meincken, M.: Inter-annual growth response of three Miombo tree species to climatic effects, Southern Forests: a Journal of Forest Science, 82, 135-147, 10.2989/20702620.2020.1814111, 2020.

Olson, D. M., Dinerstein, E., Wikramanayake, E. D., Burgess, N. D., Powell, G. V. N., Underwood, E. C., D'amico, J. A., Itoua, I., Strand, H. E., Morrison, J. C., Loucks, C. J., Allnutt, T. F., Ricketts, T. H., Kura, Y., Lamoreux, J. F., Wettengel, W. W., Hedao, P., and Kassem, K. R.: Terrestrial Ecoregions of the World: A New Map of Life on Earth: A new global map of terrestrial ecoregions provides an innovative tool for conserving biodiversity, BioScience, 51, 933-938, 10.1641/0006-3568(2001)051[0933:Teotwa]2.0.Co;2, 2001.

Pelletier, J., Paquette, A., Mbindo, K., Zimba, N., Siampale, A., Chendauka, B., Siangulube, F., and Roberts, J. W.: Carbon sink despite large deforestation in African tropical dry forests (miombo woodlands), Environmental Research Letters, 13, 094017, 2018.

Phillips, O. L., Sullivan, M. J. P., Baker, T. R., Monteagudo Mendoza, A., Vargas, P. N., and Vásquez, R.: Species Matter: Wood Density Influences Tropical Forest Biomass at Multiple Scales, Surveys in Geophysics, 40, 913-935, 10.1007/s10712-019-09540-0, 2019.

Ploton, P., Barbier, N., Momo, S. T., Réjou-Méchain, M., Boyemba Bosela, F., Chuyong, G. B., Dauby, G., Droissart, V., Fayolle, A., and Goodman, R. C.: Closing a gap in tropical forest biomass estimation: taking crown mass variation into account in pantropical allometries, Biogeosciences, 13, 1571-1585, 2016.

Poppenwimer, T.: WWF Spatial Regions [dataset], https://doi.org/10.6084/m9.figshare.20972071.v1, 2022.

Quegan, S., Le Toan, T., Chave, J., Dall, J., Exbrayat, J.-F., Minh, D. H. T., Lomas, M., D'Alessandro, M. M., Paillou, P., Papathanassiou, K., Rocca, F., Saatchi, S., Scipal, K., Shugart, H., Smallman, T. L., Soja, M. J., Tebaldini, S., Ulander, L., Villard, L., and Williams, M.: The European Space Agency BIOMASS mission: Measuring forest above-ground biomass from space, Remote Sensing of Environment, 227, 44-60, https://doi.org/10.1016/j.rse.2019.03.032, 2019.

R Core Team: _R: A Language and Environment for Statistical Computing_. R Foundation for Statistical Computing, https://www.R-project.org/, 2023.

Rathgeber, C. B., Cuny, H. E., and Fonti, P.: Biological basis of tree-ring formation: a crash course, Frontiers in Plant Science, 7, 734, 2016.

Réjou-Méchain, M., Tanguy, A., Piponiot, C., Chave, J., and Hérault, B.: biomass: an r package for estimating above-ground biomass and its uncertainty in tropical forests, Methods in Ecology and Evolution, 8, 1163-1167, https://doi.org/10.1111/2041-210X.12753, 2017.

Ribeiro, N. S., Silva de Miranda, P. L., and Timberlake, J.: Biogeography and ecology of miombo woodlands, in: Miombo woodlands in a changing environment: securing the resilience and sustainability of people and woodlands, Springer, 9-53, 2020.

Ryan, C. M., Williams, M., and Grace, J.: Above-and belowground carbon stocks in a miombo woodland landscape of Mozambique, Biotropica, 43, 423-432, 2011.

Schloerke, B., Cook, D., Larmarange, J., Briatte, F., Marbach, M., Thoen, E., Elberg, A., and Crowley, J.: GGally: Extension to 'ggplot2'. R package version 2.1.2, https://CRAN.R-project.org/package=GGally, 2021.

Sileshi, G. W.: A critical review of forest biomass estimation models, common mistakes and corrective measures, Forest Ecology and Management, 329, 237-254, 2014.

Sullivan, M. J., Lewis, S. L., Hubau, W., Qie, L., Baker, T. R., Banin, L. F., Chave, J., Cuni-Sanchez, A., Feldpausch, T. R., and Lopez-Gonzalez, G.: Field methods for sampling tree height for tropical forest biomass estimation, Methods in ecology and evolution, 9, 1179-1189, 2018.

Syampungani, S., Tigabu, M., Matakala, N., Handavu, F., and Oden, P. C.: Coppicing ability of dry miombo woodland species harvested for traditional charcoal production in Zambia: a win–win strategy for sustaining rural livelihoods and recovering a woodland ecosystem, Journal of Forestry Research, 28, 549-556, 10.1007/s11676-016-0307-1, 2017.

Terryn, L., Calders, K., Meunier, F., Bauters, M., Boeckx, P., Brede, B., Burt, A., Chave, J., da Costa, A. C. L., and D'hont, B.: New tree height allometries derived from terrestrial laser scanning reveal substantial discrepancies with forest inventory methods in tropical rainforests, Global change biology, 30, e17473, 2024.

Timberlake, J., Chidumayo, E., and Sawadogo, L.: Distribution and characteristics of African dry forests and woodlands, in: The dry forests and woodlands of Africa: managing for products

and services, edited by: Chidumayo, E. N., Gumbo, Davison J., Earthscan, London - UK, 11-41, 2010.

Wang, Y., Lehtomäki, M., Liang, X., Pyörälä, J., Kukko, A., Jaakkola, A., Liu, J., Feng, Z., Chen, R., and Hyyppä, J.: Is field-measured tree height as reliable as believed–A comparison study of tree height estimates from field measurement, airborne laser scanning and terrestrial laser scanning in a boreal forest, ISPRS Journal of Photogrammetry and Remote Sensing, 147, 132-145, 2019.

White, F.: The vegetation of Africa, Unesco, Paris1983.

Wickham, H., Averick, M., Bryan, J., Chang, W., McGowan, L. D. A., François, R., Grolemund, G., Hayes, A., Henry, L., and Hester, J.: Welcome to the Tidyverse, Journal of open source software, 4, 1686, 2019.

Wilke, C.: _cowplot: Streamlined Plot Theme and Plot Annotations for 'ggplot2'_. R package version 1.1.1, <https://CRAN.R-project.org/package=cowplot>. 2020.

Williams, M., Ryan, C., Rees, R., Sambane, E., Fernando, J., and Grace, J.: Carbon sequestration and biodiversity of re-growing miombo woodlands in Mozambique, Forest Ecology and management, 254, 145-155, 2008.

Yambayamba, A. M., Fischer, F. J., and Jucker, T.: Competition, Precipitation, and Temperature Shape Deviations From Scaling Laws in the Crown Allometries of Miombo Woodlands, Biotropica, 57, e70093, https://doi.org/10.1111/btp.70093, 2025.

Zhang, J. and Qian, H.: U.Taxonstand: An R package for standardizing scientific names of plants and animals, Plant Diversity, 45, 1-5, https://doi.org/10.1016/j.pld.2022.09.001, 2023.

Zianis, D., Muukkonen, P., Mäkipää, R., and Mencuccini, M.: Biomass and stem volume equations for tree species in Europe, Silva Fennica Monographs, 4, 1-63, 2005.